Radar Code Design for Detection of Moving Targets

Mohammad Mahdi Naghsh*, Mojtaba Soltanalian, Petre Stoica, *Fellow, IEEE* and

Mahmoud Modarres-Hashemi

Abstract

In this paper, we study the problem of pulsed-radar transmit code design for detection of moving targets in the presence of signal-dependent clutter. For unknown target Doppler shift, the optimal detector does not lead to a closed-form expression. Therefore, we resort to average and worst-case performance metrics of the optimal detector for code design. We propose several algorithms under two novel frameworks to solve highly non-convex design problems. We also consider low-peak-to-average-power ratio code design.

Keywords: Clutter, code design, moving target detection, optimal detector, peak-to-average-power ratio.

I. INTRODUCTION

Radars as well as many other active sensing systems face the simultaneous effects of signal-dependent and independent interferences. The signal-dependent interference, usually known as clutter, is the echo of the transmitted signals produced by uninteresting obstacles. On the other hand, the signal-independent interferences include various types of noise, jamming, and other unwanted emissions. Due to the difference between the target velocity and motions of the clutter scatteres, Doppler shifts of the moving targets play an important role in distinguishing the targets from clutter background. However, the target Doppler shift is usually unknown at the transmitter. Considering such an ambiguity along with the presence of clutter, and the practical implementation demands for low peak-to-average-power ratio (PAR) make the transmit code design a challenging task.

The signal design for radar performance improvement has been an active area of research in the last decades; however, the majority of previous works have considered either stationary target or clutter-free scenarios. The effect of clutter has been considered in early studies for stationary targets, or targets with known Doppler shifts (see e.g. [1]–[5]). In [6] a solution for the case of a stationary target with no clutter motion was derived; more concretely, [6] proposed a method for obtaining the spectrum of the optimal transmit signal, which is later used for the code's approximate synthesis. A related problem to that of [6] has been considered in [7] with a discrete-time model and PAR constraint (see also [8], [9]). In [10], two signal design approaches based on mutual information (MI) and signal-to-interference-plus noise ratio (SINR) metrics have been considered for stationary extended target recognition. Signal design for detection performance improvement of multiple-input multiple-output (MIMO) radars has been studied in [11] and [12] for stationary targets in the absence of clutter motion (see also [13]). Moreover, [14] considers stationary target classification for MIMO radars in white noise background. Some clutter-free scenarios are discussed in [15]–[17]. The unknown Doppler shift of the target has been taken into account in [18] and [19]. The reference [18] considers the worst-case code design problem for clutter-free cases under a similarity constraint to a given code. The ideas of [18] are generalized in [19] where the PAR constraint is included.

In this paper, we study the problem of radar signal design for detection of a moving target in the presence of clutter. Two different design methodologies including *average* and *worst-case* approaches are considered to handle the fact that the Doppler shift of the target is often unknown at the transmit side. The corresponding optimization problems are highly non-convex. To tackle these problems, we propose several novel algorithms under two frameworks for unconstrained and constrained design. Particularly, we introduce the **Co**nvexification via **Re**parametrization (CoRe) framework which considers a relaxation of the original design problem to a core semi-definite program (SDP), that we call CSDP. The CSDP is then followed by a code synthesis stage. Moreover, another framework based on a **C**yclic **A**lgorithm for **D**irect **CO**de **DE**sign (which we call CADCODE) is proposed to carry out a direct code design via cyclic minimization. The key contributions of this paper are:

- The simultaneous presence of clutter (i.e. the signal-dependent interference) and the unknown Doppler shift of the moving targets is considered. To the best of our knowledge, designing codes for improving detection performance in such cases has not been addressed in the literature prior to this work.

- To deal with the unknown Doppler shift of the target, both average and worst-case performance

metrics of the optimal detector (with known Doppler shift) are considered for code design. The connections between the considered metrics and the detection performance are also addressed. As a result, the proposed code design schemes enable the user with the possibility to choose the desired performance guarantees (at any occurred scenario) freely.

- The PAR constraint is taken into account in the code design. Several extensions of the proposed methods are derived to handle such constrained code design problems.

- Using the CSDP solution in the CoRe framework, computational upper bounds on the achievable values of the average and worst-case performance metrics are provided. The obtained upper bounds can be used as benchmarks to examine the goodness of codes obtained by different code design methods. In addition, they provide the system designers with a better insight into the optimal system performance in various scenarios.

The rest of this paper is organized as follows. In Section II, we present the data modeling and derive the optimal detectors for both known and unknown target Doppler shift. The average design is studied in Section III. This section also includes a presentation of the CoRe and CADCODE frameworks. Section IV is dedicated to the worst-case code design. The PAR constrained code design is considered in Section V. Several numerical examples are provided in Section VI. Finally, Section VII concludes the paper.

Notation: We use bold lowercase letters for vectors and bold uppercase letters for matrices. $(\cdot)^T$, $(\cdot)^*$ and $(\cdot)^H$ denote the vector/matrix transpose, the complex conjugate, and the Hermitian transpose, respectively. $\mathbf{I}_N$ represents the identity matrix in $\mathbb{C}^{N \times N}$. $\mathbf{1}$ and $\mathbf{0}$ are the all-one and the all-zero vectors/matrices. $\mathbf{e}_k$ is the kth standard basis vector in $\mathbb{C}^N$. The Frobenius norm of a matrix $\mathbf{X}$ (denoted by $\|\mathbf{X}\|_F$) with entries $\{X_{k,l}\}$ is equal to $\left(\sum_{k,l} |X_{k,l}|^2 \right)^{\frac{1}{2}}$. The l_2-norm of a vector $\mathbf{x}$ is denoted by $\|\mathbf{x}\|$. The symbol $\odot$ stands for the Hadamard (element-wise) product of matrices. $\mathrm{tr}(\cdot)$ is the trace of a square matrix argument. The notations $\lambda_{max}(\cdot)$ and $\lambda_{min}(\cdot)$ indicate the principal and the minor eigenvalues of a Hermitian matrix, respectively. $\mathbf{Diag}(\cdot)$ denotes the diagonal matrix formed by the entries of the vector argument, whereas $\mathbf{diag}(\cdot)$ denotes the vector formed by collecting the diagonal entries of the matrix argument. $\mathrm{E}\{\cdot\}$ stands for the statistical expectation operator. We write $\mathbf{A} \succeq \mathbf{B}$ iff $\mathbf{A} - \mathbf{B}$ is positive semi-definite, and $\mathbf{A} \succ \mathbf{B}$ iff $\mathbf{A} - \mathbf{B}$ is positive-definite. Finally, $\Re(\cdot)$ and $\arg(\cdot)$ denote the real-part and the phase angle (in radians) of the complex-valued argument.

II. DATA MODELING AND OPTIMAL DETECTOR

A. Data Modeling

We consider a narrow-band pulsed-radar system using a train of pulses. The baseband transmit signal can be formulated as

$$s(t) = \sum_{n=0}^{N-1} a_n \, \phi(t - nT_{PRI}) \tag{1}$$

where $\phi(.)$ is the basic unit-energy transmit pulse (with time duration τ_p), T_{PRI} is the pulse repetition interval ($T_{PRI} \gg \tau_p$), and $\{a_n\}_{n=0}^{N-1}$ are the weights that are to be optimally designed.

At the transmitter, the baseband signal is modulated by a carrier frequency ω_c. The backscattered signal from a point-like moving target can be expressed as

$$r(t) = \alpha_t s(t - \tau) e^{j(\omega_c + \nu)(t-\tau)} + c(t) + w(t) \tag{2}$$

where α_t is the amplitude of the target echo (accounting for target reflectivity and channel effects), τ and ν denote the target delay and Doppler shift, respectively, $c(t)$ is the clutter component, and $w(t)$ represents the signal-independent interferences.

We assume that both $c(t)$ and $w(t)$ are Gaussian random processes. In particular, we assume that the clutter component is the signal echo produced by many individual point scatterers (distributed across the delay and Doppler domains) which are statistically independent. Under such an assumption, $c(t)$ can be formulated as [2]

$$c(t) = \sum_{k=1}^{N_{\mathrm{ct}}} \sum_{l=1}^{N_{\mathrm{cd}}} \rho_{kl} s(t - \tau_k) e^{j(\omega_c + \omega_l)(t - \tau_k)} \tag{3}$$

where N_{ct} and N_{cd} are the number of clutter scatterers in the delay and Doppler domains[1], respectively, and ρ_{kl} is the amplitude of a specific clutter scatterer at time delay τ_k and Doppler shift ω_l (due to the clutter motion).

Note that in radar applications, the pulse $\phi(t)$ and its time-shifted versions can be used as an orthonormal basis for signal recovery at the receiver. More precisely, the matched filter $\phi^*(-t)$ is usually applied to the downconverted received signal (i.e. $r(t)e^{-j\omega_c t}$) and the output of the matched filter is then sampled at the time delays corresponding to the range-cell under test, i.e. $t = nT_{PRI} + \tau$ for $0 \leq n \leq N - 1$. The discrete-time received signal $\mathbf{r}$ for the range-cell corresponding to the time delay τ can be written

---

[1]It is assumed that the number of the independent scatterers is sufficiently large such that the central limit theorem holds and the Gaussian distribution for $c(t)$ can be justified (see e.g., [2] [20] [21]).

as (see Appendix A for a derivation)

$$\mathbf{r} = \alpha\,\mathbf{a} \odot \mathbf{p} + \mathbf{a} \odot \mathbf{c} + \mathbf{w} \qquad (4)$$

where $\alpha = \alpha_t e^{-j\omega_c\tau}$, $\mathbf{a} \triangleq [a_0 \ a_1 \ \ldots \ a_{N-1}]^T$ is the code vector (to be designed), $\mathbf{p} \triangleq [1 \ e^{j\omega} \ \ldots \ e^{j(N-1)\omega}]^T$ with ω being the normalized Doppler shift of the target, $\mathbf{c}$ is the vector corresponding to the clutter component, and the vector $\mathbf{w}$ represents the signal-independent interferences[2]. A detailed construction of $\mathbf{c}$ and $\mathbf{w}$ from the continuous variables $c(t)$ and $w(t)$ can also be found in Appendix A. Herein we remark on the fact that (4) refers to the cases with unambiguous clutter scatterers.

Using (4), the target detection problem can be cast as the following binary hypothesis test:

$$\begin{cases} \text{H}_0: & \mathbf{r} = \mathbf{a} \odot \mathbf{c} + \mathbf{w} \\ \text{H}_1: & \mathbf{r} = \alpha\mathbf{a} \odot \mathbf{p} + \mathbf{a} \odot \mathbf{c} + \mathbf{w} \end{cases} \qquad (5)$$

Note that the covariance matrices of $\mathbf{c}$ and $\mathbf{w}$ (denoted by $\mathbf{C}$ and $\mathbf{M}$) can be assumed to be priori known (e.g. they can be obtained by using geographical, meteorological, or pre-scan information) [23] [22]. As to the target, we assume α is a zero-mean complex Gaussian random variable with variance σ_T^2 (i.e. Swerling-I model).

B. Optimal Detector for a priori known Doppler shift

Let $\mathbf{x} = \mathbf{D}^{-1/2}\mathbf{r}$ with $\mathbf{D} = \mathbf{M} + \mathbf{A}\mathbf{C}\mathbf{A}^H$, and $\mathbf{A} = \text{Diag}(\mathbf{a})$ (that is referred to as *code matrix* in the sequel). The detection problem in (5) can equivalently be expressed in terms of $\mathbf{x}$. More precisely, for a known target Doppler shift, the problem in (5) is equivalent to:

$$\begin{cases} \text{H}_0: & \mathbf{x} \sim \mathcal{CN}(\mathbf{0}, \mathbf{I}) \\ \text{H}_1: & \mathbf{x} \sim \mathcal{CN}(\mathbf{0}, \mathbf{S} + \mathbf{I}) \end{cases} \qquad (6)$$

where $\mathbf{S} = \sigma_T^2 \mathbf{D}^{-1/2}(\mathbf{a}\odot\mathbf{p})(\mathbf{a}\odot\mathbf{p})^H \mathbf{D}^{-1/2}$. The optimal detector compares the likelihood-ratio associated with the above problem, i.e. the ratio of the pdf of $\mathbf{x}$ under H_1 over that of H_0, with a detection threshold. According to (6), the likelihood-ratio for the problem is given by

$$\mathcal{L}(\mathbf{x}) = \frac{1}{\det(\mathbf{S} + \mathbf{I})} \left(\frac{\exp\left(-\mathbf{x}^H(\mathbf{S} + \mathbf{I})^{-1}\mathbf{x}\right)}{\exp\left(-\mathbf{x}^H\mathbf{x}\right)} \right). \qquad (7)$$

---

[2]Note that in the data model (4) we neglect the effects of the antenna pattern; however, the results can be straightforwardly extended to include these effects (see e.g. [22]).

By taking logarithm and removing the constants, the following expression is obtained for the optimal detector:

$$|\mathbf{r}^H \left(\mathbf{M} + \mathbf{ACA}^H\right)^{-1} (\mathbf{a} \odot \mathbf{p})|^2 \underset{\mathrm{H}_1}{\overset{\mathrm{H}_0}{\gtrless}} \eta \tag{8}$$

where η is the detection threshold. Note that the above detector is nothing but a whitening process, a matched filtering, and a square-law detection. The performance of the above detector depends on the following SNR [24, Chapter 8]

$$\lambda = \sigma_T^2 (\mathbf{a} \odot \mathbf{p})^H \left(\mathbf{M} + \mathbf{ACA}^H\right)^{-1} (\mathbf{a} \odot \mathbf{p}). \tag{9}$$

It is interesting to observe that the above performance metric is invariant to a phase-shift of the code vector $\mathbf{a}$, i.e. the code vectors $\mathbf{a}$ and $e^{j\varphi}\mathbf{a}$ (for any $\varphi \in [0, 2\pi]$) result in the same value of the SNR.

C. Optimal Detector for an unknown Doppler shift

The target Doppler shift ω is usually unknown at the transmitter. In such cases, the detector of (8) does not hold true anymore. The optimal detector for the detection problem in (5) in cases where ω is unknown is obtained by considering the pdf of ω. The distribution of the vector $\mathbf{r}$ (and $\mathbf{x}$) are no longer Gaussian under H_1 and the optimal detector does not lead to a closed-form expression. More precisely, let $f(\omega)$ denote the pdf of ω. The optimal detector is obtained by considering the average likelihood-ratio [24]:

$$\mathcal{L}(\mathbf{x}) = \int_\Omega \mathcal{L}(\mathbf{x}|\omega) f(\omega) \, d\omega \tag{10}$$

which results in the following detector [25]

$$\int_\Omega \frac{1}{1+\lambda} \exp\left(\frac{\sigma_T^2 \mathbf{r}^H \mathbf{D}^{-1} (\mathbf{a} \odot \mathbf{p})(\mathbf{a} \odot \mathbf{p})^H \mathbf{D}^{-1} \mathbf{r}}{1+\lambda}\right) f(\omega) \, d\omega \underset{\mathrm{H}_1}{\overset{\mathrm{H}_0}{\gtrless}} \eta' \tag{11}$$

where $\Omega = [\omega_l, \omega_u]$ denotes the considered interval for the target Doppler shift[3] ω and λ is given by (9). It is worth mentioning that the values of ω_l and ω_u and the pdf of ω can be obtained in practice using prior knowledge about the type of target (e.g. knowing if the target is an airplane, a ship, or a missile), rough estimates of the target Doppler shift obtained by pre-scan procedures, and employing cognitive methods [23] [26]. Usually, a uniform distribution for ω is considered over Ω to model the uncertainty of the target Doppler shift [22].

---

[3]Note that Ω can also be the union of several intervals.

III. CODE DESIGN IN AVERAGE SENSE

Code design to improve the detection performance of the system for a known target Doppler shift ω can be accomplished by the maximization of the following performance metric[4] for a given ω:

$$(\mathbf{a} \odot \mathbf{p})^H \left(\mathbf{M} + \mathbf{ACA}^H\right)^{-1} (\mathbf{a} \odot \mathbf{p}) \tag{12}$$

$$= \mathrm{tr}\left\{\mathbf{A}^H(\mathbf{M} + \mathbf{ACA}^H)^{-1}\mathbf{App}^H\right\}$$

$$= \mathrm{tr}\left\{\left((\mathbf{A}^H\mathbf{M}^{-1}\mathbf{A})^{-1} + \mathbf{C}\right)^{-1}\mathbf{pp}^H\right\}.$$

In cases where target Doppler shift is unknown, the expressions for the corresponding optimal detector and its performance metrics are too complicated to be used for code design (see also [27] [28]). In such a circumstance, we consider the following design metric (referred to as average metric):

$$\mathrm{tr}\left\{\left(\mathbf{A}^{-1}\mathbf{MA}^{-H} + \mathbf{C}\right)^{-1}\mathbf{W}\right\} \tag{13}$$

where $\mathbf{W} = \mathrm{E}\{\mathbf{pp}^H\}$. The mathematical background for selection of such metric is as follows: It can be shown (see below) that maximizing the above metric results in maximization of a lower bound on the J-divergence [29] associated with the detection problem in (5) for unknown ω. Furthermore, for large SNR regimes, maximization of the above metric approximates well the maximization of the J-divergence. More precisely, the J-divergence associated with the binary hypothesis test is given by [27]

$$\mathcal{J} = \mathrm{E}\{\log(\mathcal{L}(\mathbf{x}))|\mathrm{H}_1\} - \mathrm{E}\{\log(\mathcal{L}(\mathbf{x}))|\mathrm{H}_0\}. \tag{14}$$

Therefore, for the detection problem in (5) in cases where ω is unknown we can write

$$\mathcal{J} = E\{\mathcal{J}|\omega\}. \tag{15}$$

For a given ω, the detection problems in (5) and (6) are equivalent, and hence $\mathcal{J}|\omega$ can be derived considering (6) as:

$$\mathcal{J}|\omega = \left(-\log\left(1 + \lambda\right) + \frac{\lambda^2 + \lambda}{1 + \lambda}\right) - \left(-\log\left(1 + \lambda\right) + \frac{\lambda}{1 + \lambda}\right) = \frac{\lambda^2}{1 + \lambda} \tag{16}$$

---

[4]In what follows, we assume that all the code elements are non-zero.

where λ is defined in (9). Now observe that $g(x) = x^2/(1+x)$ is a convex function. Consequently, using Jensen inequality we conclude

$$\mathcal{J} = \mathrm{E}\left\{\frac{\lambda^2}{1+\lambda}\right\} \geq \underbrace{\frac{(\mathrm{E}\{\lambda\})^2}{1+\mathrm{E}\{\lambda\}}}_{\mathcal{J}_{LB}}. \tag{17}$$

Furthermore, $g(x) = x^2/(1+x)$ is a monotonically increasing function. As a result, maximization of the $\mathrm{E}\{\lambda\}$ leads to maximization of the $\mathcal{J}_{LB}$ in the above inequality. Owing to the fact that the considered metric in (13) is equal to $\mathrm{E}\{\lambda\}$, the maximization of the average metric leads to maximization of the lower bound $\mathcal{J}_{LB}$ on the J-divergence $\mathcal{J}$. An analysis of the tightness of the bound $\mathcal{J}_{LB}$ is presented in Appendix B. The J-divergence has an asymptotic relationship with the detection performance of a hypothesis test and can also be considered as a bound on the detection performance [30] [29].

Remark 1: Note that $\mathcal{J} = \mathrm{E}\left\{\lambda - 1 + \frac{1}{\lambda+1}\right\}$ and hence for large SNR, i.e. large λ, we have $\mathcal{J} \approx \mathrm{E}\{\lambda\} - 1$. As a result, in such cases, maximization of the considered average metric approximates well the maximization of the J-divergence. A similar approximation has also been used in [30] for radar signal design. With similar calculations, for small λ, it can be shown that maximization of the average metric is approximately equivalent to maximization of the Mutual Information associated with the problem (5) (that is given by $\mathrm{E}\{\log(1+\lambda)\}$). For known ω, the average metric is identical to the performance metric in (12) and directly determines the performance of the optimal detector. ∎

To optimize the detection performance, the average metric (13) can be maximized under an energy constraint:

$$\max_{\mathbf{A}} \quad \mathrm{tr}\left\{\left(\mathbf{A}^{-1}\mathbf{M}\mathbf{A}^{-H} + \mathbf{C}\right)^{-1}\mathbf{W}\right\} \tag{18}$$
$$\text{subject to} \quad \mathrm{tr}\left\{\mathbf{A}\mathbf{A}^{H}\right\} \leq e$$

where e denotes the maximum energy that can be used for transmission. Note that if $\mathbf{A}$ is claimed to be a solution to (18) with $\mathrm{tr}\{\mathbf{A}\mathbf{A}^{H}\} < e$, then $\gamma\mathbf{A}$ (for some $\gamma > 1$ such that $\gamma\,\mathrm{tr}\{\mathbf{A}\mathbf{A}^{H}\} = e$) is feasible but leads to a larger value of the objective function. Therefore, the energy constraint in (18) is active. In the following, we propose two different frameworks to tackle the code optimization problem in (18).

A. Convexification via Reparametrization (CoRe)

First, we introduce the CoRe framework which is based on a relaxation of the optimization problem in (18). In particular, we show that a relaxed version of the code design problem in (18) can be formulated

as an SDP. Let

$$\mathbf{X} \triangleq \mathbf{A}^H \mathbf{M}^{-1} \mathbf{A} \tag{19}$$

and observe that $\mathbf{X} \succ \mathbf{0}$. The energy constraint of (18) can be rewritten noting that

$$\mathrm{tr}\{\mathbf{X}\} = \mathrm{tr}\{\mathbf{A}^H \mathbf{M}^{-1} \mathbf{A}\} = \sum_{k=1}^{N} m_{kk} |a_k|^2 \tag{20}$$

where $\{m_{kk}\}_{k=1}^{N}$ are the diagonal entries of the positive-definite matrix $\mathbf{M}^{-1}$. Using (20), the energy of the code can be alternatively written as

$$\mathrm{tr}\{\mathbf{A}^H \mathbf{A}\} = \mathrm{tr}\{\mathbf{X}\mathbf{G}\} \tag{21}$$

where $\mathbf{G} \triangleq (\mathbf{M}^{-1} \odot \mathbf{I})^{-1}$ is a diagonal matrix with diagonal entries $\{1/m_{kk}\}_{k=1}^{N}$.

Next, we reformulate (18) as a convex optimization problem w.r.t. $\mathbf{X}$. Note that there exists $\mathbf{B} \in \mathbb{C}^{N \times N}$ such that $\mathbf{C} = \mathbf{B}\mathbf{B}^H$. Using the matrix inversion lemma we have that

$$(\mathbf{X}^{-1} + \mathbf{C})^{-1} = \mathbf{X} - \mathbf{X}\mathbf{B}(\mathbf{I} + \mathbf{B}^H \mathbf{X}\mathbf{B})^{-1}\mathbf{B}^H \mathbf{X}. \tag{22}$$

Let $\delta = \mathrm{rank}(\mathbf{W})$, and let $\mathbf{W} = \sum_{k=1}^{\delta} \mathbf{w}_k \mathbf{w}_k^H$. As a result,

$$\mathrm{tr}\left\{ \left(\mathbf{A}^{-1}\mathbf{M}\mathbf{A}^{-H} + \mathbf{C}\right)^{-1} \mathbf{W} \right\} = \mathrm{tr}\left\{ (\mathbf{X}^{-1} + \mathbf{C})^{-1}\mathbf{W} \right\} \tag{23}$$
$$= \sum_{k=1}^{\delta} \left\{ \mathbf{w}_k^H \mathbf{X}\mathbf{w}_k - \mathbf{w}_k^H \mathbf{X}\mathbf{B}(\mathbf{I} + \mathbf{B}^H \mathbf{X}\mathbf{B})^{-1}\mathbf{B}^H \mathbf{X}\mathbf{w}_k \right\}.$$

To maximize (23), each term in the latter summation can be dealt with by means of a linear matrix inequality (LMI) using auxiliary variables $\{\beta_k\}$:

$$\beta_k \geq -\mathbf{w}_k^H \mathbf{X}\mathbf{w}_k + \mathbf{w}_k^H \mathbf{X}\mathbf{B}(\mathbf{I} + \mathbf{B}^H \mathbf{X}\mathbf{B})^{-1}\mathbf{B}^H \mathbf{X}\mathbf{w}_k \tag{24}$$
$$\Leftrightarrow \begin{bmatrix} \beta_k + \mathbf{w}_k^H \mathbf{X}\mathbf{w}_k & \mathbf{w}_k^H \mathbf{X}\mathbf{B} \\ \mathbf{B}^H \mathbf{X}\mathbf{w}_k & \mathbf{I} + \mathbf{B}^H \mathbf{X}\mathbf{B} \end{bmatrix} \succeq \mathbf{0}.$$

In light of Eqs. (21) and (23), and the LMIs introduced in (24), the optimization problem (18) boils

down (in a relaxed form) to the following core SDP (CSDP):

$$\text{CSDP:} \quad \min_{\mathbf{X}, \{\beta_k\}_{k=1}^{\delta}} \quad \sum_{k=1}^{\delta} \beta_k \tag{25}$$

subject to

$$\begin{bmatrix} \beta_k + \mathbf{w}_k^H \mathbf{X} \mathbf{w}_k & \mathbf{w}_k^H \mathbf{X} \mathbf{B} \\ \mathbf{B}^H \mathbf{X} \mathbf{w}_k & \mathbf{I} + \mathbf{B}^H \mathbf{X} \mathbf{B} \end{bmatrix} \succeq \mathbf{0}, \quad \forall\, k,$$

$$\text{tr}\{\mathbf{X}\mathbf{G}\} \le e,$$

$$\mathbf{X} \succ \mathbf{0}.$$

Note that the above CSDP can be solved in polynomial-time (e.g. see [31] in which an $O(N^{3.5})$-complexity algorithm is introduced to solve such SDPs). The global optimum $\mathbf{X}$ of the above CSDP can be used to synthesize the code matrix $\mathbf{A}$. To obtain $\mathbf{A}$ such that $\mathbf{A}^H \mathbf{M}^{-1} \mathbf{A} \cong \mathbf{X}$, we consider the optimization problem

$$\min_{\mathbf{A}, \mathbf{Q}} \quad \|\mathbf{X}^{1/2} \mathbf{Q} - \mathbf{A}^H \mathbf{M}^{-1/2}\|_F^2 \tag{26}$$

$$\text{subject to} \quad \mathbf{Q}\mathbf{Q}^H = \mathbf{I}$$

where $\mathbf{Q}$ is an auxiliary matrix. In the following, we propose an efficient cyclic algorithm for solving (26). For any fixed code matrix $\mathbf{A}$, (26) leads to the maximization problem:

$$\max_{\mathbf{Q}} \quad \Re\left(\text{tr}\left\{\mathbf{X}^{1/2} \mathbf{Q} \mathbf{M}^{-1/2} \mathbf{A}\right\}\right) \tag{27}$$

$$\text{subject to} \quad \mathbf{Q}\mathbf{Q}^H = \mathbf{I}.$$

Interestingly, a similar problem to (27) has been studied in [32] where an explicit solution was derived. Let $\mathbf{V}_1 \mathbf{S} \mathbf{V}_2^H$ represent the singular value decomposition (SVD) of $\mathbf{M}^{-1/2} \mathbf{A} \mathbf{X}^{1/2}$. Then the explicit solution of (27) is given by $\mathbf{V}_2 \mathbf{V}_1^H$ (see [32] for details). Furthermore, for fixed $\mathbf{Q}$, the solution of (26) w.r.t. the code matrix $\mathbf{A}$ can be obtained solving the problem:

$$\min_{\mathbf{A}} \quad \text{tr}\left\{\mathbf{A}^H \mathbf{M}^{-1} \mathbf{A}\right\} - 2\Re\left(\text{tr}\left\{\mathbf{X}^{1/2} \mathbf{Q} \mathbf{M}^{-1/2} \mathbf{A}\right\}\right) \tag{28}$$

which can be rewritten (in vectorized form) as

$$\min_{\mathbf{a}} \quad \mathbf{a}^H(\mathbf{M}^{-1} \odot \mathbf{I})\mathbf{a} - 2\Re(\mathbf{b}^H \mathbf{a}) \tag{29}$$

with $\mathbf{b} \triangleq \mathrm{diag}(\mathbf{X}^{1/2}\mathbf{Q}^*\mathbf{M}^{-1/2})$. The solution $\mathbf{a}$ of (29) is given by

$$\mathbf{a} = (\mathbf{M}^{-1} \odot \mathbf{I})^{-1}\mathbf{b} = \mathbf{G}\mathbf{b}. \tag{30}$$

Remark 2: Note that the aim of the synthesis problem (26) is to provide $\mathbf{A}$ such that $\mathbf{A}^H\mathbf{M}^{-1}\mathbf{A} \cong \mathbf{X}$, and also that an energy constraint has already been imposed when obtaining the $\mathbf{X}$ (see (25)). Therefore, in (26), we do not consider the energy constraint, as it has been implicitly imposed. However, one might be interested to explicitly consider the energy constraint in (26). In this case, the optimization problem for fixed $\mathbf{Q}$ is convex w.r.t. $\mathbf{A}$ and hence can be solved efficiently (but (30) does not hold). Note that it was numerically observed that the difference between explicitly imposing the energy constraint in (26) and the considered synthesis problem in the paper is very minor. ∎

The steps of the CoRe framework are summarized in Table I. It is worth mentioning that as the solution $\mathbf{X}$ to the CSDP does not necessarily possess the desired structure in (19), some degradation of the metric in (13) can be expected at the synthesis stage. In other words, the CSDP solution in (25) provides an upper bound on the average metric. This upper bound can be used to assess the quality of code design methods as well as the system performance in various scenarios.

TABLE I

CoRe for Optimal Code Design Using the Average Metric

Step 1: Solve the CSDP of (25) to obtain its global optimum $\mathbf{X}$.
Step 2 *(The synthesis stage)*: Initialize $\mathbf{a}$ with a random vector in $\mathbb{C}^N$.
Step 2-1: Compute $\mathbf{Q} = \mathbf{V}_2\mathbf{V}_1^H$ where $\mathbf{V}_1\mathbf{S}\mathbf{V}_2^H$ represents the SVD of $\mathbf{M}^{-1/2}\mathbf{A}\mathbf{X}^{1/2}$.
Step 2-2: Compute $\mathbf{a} = \mathbf{G}\,\mathrm{diag}(\mathbf{X}^{1/2}(\mathbf{Q}^*)\mathbf{M}^{-1/2})$.
Step 2-3: Repeat steps 2-1 and 2-2 until a pre-defined stop criterion is satisfied, e.g. $\|\mathbf{a}^{(k+1)} - \mathbf{a}^{(k)}\| \le \epsilon$ for some $\epsilon > 0$, where the superscript k denotes the iteration number.

B. Cyclic Algorithm for Direct COde DEsign (CADCODE)

In this sub-section, we propose the CADCODE framework for solving (18) directly w.r.t. the code matrix $\mathbf{A}$.

We begin by noting that as $\mathbf{W} \succeq \mathbf{0}$ there must exist a full column-rank matrix $\mathbf{V} \in \mathbb{C}^{N \times \delta}$ such that $\mathbf{W} = \mathbf{V}\mathbf{V}^H$ (particularly observe that $\mathbf{V} = [\mathbf{w}_1 \ \mathbf{w}_2 \ ... \ \mathbf{w}_\delta]$ yields such decomposition of $\mathbf{W}$). As a

result,

$$
\begin{aligned}
\operatorname{tr}\left\{\left((\mathbf{A}^H \mathbf{M}^{-1} \mathbf{A})^{-1} + \mathbf{C}\right)\mathbf{W}\right\} &= \operatorname{tr}\left\{\mathbf{A}^H (\mathbf{M} + \mathbf{A}\mathbf{C}\mathbf{A}^H)^{-1}\mathbf{A}\mathbf{W}\right\} \quad (31) \\
&= \operatorname{tr}\left\{\mathbf{V}^H \mathbf{A}^H (\mathbf{M} + \mathbf{A}\mathbf{C}\mathbf{A}^H)^{-1}\mathbf{A}\mathbf{V}\right\}.
\end{aligned}
$$

Let $\boldsymbol{\Theta} \triangleq \theta\mathbf{I} - \mathbf{V}^H \mathbf{A}^H (\mathbf{M} + \mathbf{A}\mathbf{C}\mathbf{A}^H)^{-1}\mathbf{A}\mathbf{V}$ with a sufficiently large θ such that $\boldsymbol{\Theta} \succ \mathbf{0}$ (a detailed calculation of the diagonal loading parameter θ can be found in Appendix C). Note that the optimization problem (18) is equivalent to the minimization problem

$$
\begin{aligned}
\min_{\mathbf{A}} \quad & \operatorname{tr}\{\boldsymbol{\Theta}\} \quad (32) \\
\text{subject to} \quad & \operatorname{tr}\{\mathbf{A}^H \mathbf{A}\} \le e.
\end{aligned}
$$

Now define

$$
\mathbf{R} \triangleq \begin{bmatrix} \theta\mathbf{I} & \mathbf{V}^H \mathbf{A}^H \\ \mathbf{A}\mathbf{V} & \mathbf{M} + \mathbf{A}\mathbf{C}\mathbf{A}^H \end{bmatrix} \quad (33)
$$

and observe that for $\mathbf{U} \triangleq [\mathbf{I}_\delta \ \ \mathbf{0}_{N\times\delta}]^T$ we have

$$
\mathbf{U}^H \mathbf{R}^{-1} \mathbf{U} = \boldsymbol{\Theta}^{-1}. \quad (34)
$$

To tackle (32) let $g(\mathbf{A}, \mathbf{Y}) \triangleq \operatorname{tr}\{\mathbf{Y}^H \mathbf{R}\mathbf{Y}\}$ (with $\mathbf{Y}$ being an auxiliary variable), and consider the following minimization problem:

$$
\begin{aligned}
\min_{\mathbf{A}, \mathbf{Y}} \quad & g(\mathbf{A}, \mathbf{Y}) \quad (35) \\
\text{subject to} \quad & \mathbf{Y}^H \mathbf{U} = \mathbf{I} \\
& \operatorname{tr}\{\mathbf{A}^H \mathbf{A}\} \le e.
\end{aligned}
$$

For fixed $\mathbf{A}$, the minimizer $\mathbf{Y}$ of (35) can be obtained using Result 35 in [33, p. 354] as

$$
\mathbf{Y} = \mathbf{R}^{-1}\mathbf{U}(\mathbf{U}^H \mathbf{R}^{-1}\mathbf{U})^{-1}. \quad (36)
$$

On the other hand, for fixed $\mathbf{Y}$, the minimization of $g(\mathbf{Y}, \mathbf{A})$ w.r.t. $\mathbf{A}$ yields the following convex quadratically-constrained quadratic program (QCQP):

$$
\begin{aligned}
\min_{\mathbf{a}} \quad & \mathbf{a}^H\left((\mathbf{Y}_2\mathbf{Y}_2^H)\odot\mathbf{C}^T\right)\mathbf{a} + 2\Re(\mathbf{d}^H\mathbf{a}) \quad (37) \\
\text{subject to} \quad & \mathbf{a}^H\mathbf{a} \le e
\end{aligned}
$$

where $\mathbf{Y} \triangleq [\mathbf{Y}_{1\ \delta\times\delta}\ \ \mathbf{Y}_{2\ N\times\delta}]^T$ and $\mathbf{d} \triangleq \mathrm{diag}(\mathbf{V}^*\mathbf{Y}_1^*\mathbf{Y}_2^T)$. Note that the positive semi-definiteness of $(\mathbf{Y}_2\mathbf{Y}_2^H) \odot \mathbf{C}^T$ guarantees the convexity of (37). The QCQP in (37) can be solved efficiently using the Lagrange multiplier method (see Appendix D).

It is straightforward to verify that at the minimizer $\mathbf{Y}$ of (35),

$$g(\mathbf{Y}, \mathbf{A}) = \mathrm{tr}\{\boldsymbol{\Theta}\}. \tag{38}$$

From this property, we conclude that each step of the cyclic minimization of (35) leads to a decrease of $\mathrm{tr}\{\boldsymbol{\Theta}\}$. Indeed, let $f(\mathbf{A}) = \mathrm{tr}\{\boldsymbol{\Theta}\}$ and note that

$$\begin{aligned} f\left(\mathbf{A}^{(k+1)}\right) &= g\left(\mathbf{Y}^{(k+2)}, \mathbf{A}^{(k+1)}\right) \\ &\leq g\left(\mathbf{Y}^{(k+1)}, \mathbf{A}^{(k+1)}\right) \\ &\leq g\left(\mathbf{Y}^{(k+1)}, \mathbf{A}^{(k)}\right) = f\left(\mathbf{A}^{(k)}\right) \end{aligned} \tag{39}$$

where the superscript k denotes the iteration number. The first and the second inequality in (39) hold true due to the minimization of $g(\mathbf{A}, \mathbf{Y})$ w.r.t. $\mathbf{Y}$ and $\mathbf{A}$, respectively. As a result, *CADCODE converges to a stationary point of (18).* It is worth noting that the minimization steps of CADCODE (which are summarized in Table II) are solved either analytically or using standard interior-point methods [34].

TABLE II
CADCODE FOR OPTIMAL CODE DESIGN USING THE AVERAGE METRIC

Step 0: Initialize the code vector $\mathbf{a}$ using a random vector in $\mathbb{C}^N$, and form $\mathbf{R}$ as defined in (33).
Step 1: Compute $\mathbf{Y} = \mathbf{R}^{-1}\mathbf{U}(\mathbf{U}^H\mathbf{R}^{-1}\mathbf{U})^{-1}$.
Step 2: Solve the optimization problem (37) to obtain the code vector $\mathbf{a}$.
Step 3: Repeat steps 1 and 2 until a pre-defined stop criterion is satisfied, e.g. $\|\mathbf{a}^{(k+1)} - \mathbf{a}^{(k)}\| \leq \epsilon$ for some $\epsilon > 0$, where k denotes the iteration number.

IV. WORST-CASE DESIGN

Following the optimization schemes proposed for code design in the average-sense, we extend our derivations in order to handle the unknown Doppler shift of the target in a *worst-case* scenario. The worst-case approach has been considered in [18] and [19] for clutter-free scenarios. These works also address the connection between the worst-case metric and the detection performance (see also [35] for a

related problem). Considering the performance metric of the detector (8), the *worst-case metric* (for an unknown Doppler shift in the interval $[\omega_l, \omega_u]$) is defined as

$$\min_{\omega_l \leq \omega \leq \omega_u} \quad \mathrm{tr}\left\{ \left((\mathbf{A}^H \mathbf{M}^{-1} \mathbf{A})^{-1} + \mathbf{C} \right)^{-1} \mathbf{p}\mathbf{p}^H \right\}. \tag{40}$$

The maximization of the worst-case metric boils down to the max-min problem:

$$\max_{\mathbf{A}} \min_{\omega_l \leq \omega \leq \omega_u} \quad \mathrm{tr}\left\{ \left((\mathbf{A}^H \mathbf{M}^{-1} \mathbf{A})^{-1} + \mathbf{C} \right)^{-1} \mathbf{p}\mathbf{p}^H \right\} \tag{41}$$
$$\text{subject to} \quad \mathrm{tr}\left\{ \mathbf{A}^H \mathbf{A} \right\} \leq e$$

which can be rewritten (using a slack variable t) as

$$\max_{\mathbf{A}, t} \quad \{t\} \tag{42}$$

subject to

$$\mathrm{tr}\left\{ \left((\mathbf{A}^H \mathbf{M}^{-1} \mathbf{A})^{-1} + \mathbf{C} \right)^{-1} \mathbf{p}\mathbf{p}^H \right\} - t \geq 0, \quad \forall \ \omega \in [\omega_l, \omega_u],$$
$$\mathrm{tr}\left\{ \mathbf{A}^H \mathbf{A} \right\} \leq e.$$

Note that (42) is a non-convex optimization problem with infinitely many nonlinear constraints. In the following, we make use of an extension of the CoRe framework to tackle (42).

Using a new variable $\mathbf{Z} = \left((\mathbf{A}^H \mathbf{M}^{-1} \mathbf{A})^{-1} + \mathbf{C} \right)^{-1}$, one can recast (42) (in a relaxed form) as

$$\max_{\mathbf{Z}, t} \quad \{t\} \tag{43}$$

subject to

$$\mathbf{p}^H \mathbf{Z} \mathbf{p} - t \geq 0, \quad \forall \ \omega \in [\omega_l, \omega_u], \tag{44}$$

$$\mathrm{tr}\left\{ (\mathbf{Z}^{-1} - \mathbf{C})^{-1} \mathbf{G} \right\} \leq e. \tag{45}$$

Observe that for any $\omega \in [\omega_l, \omega_u]$, the constraint (44) is equivalent to

$$h(\omega) \triangleq z_0 - t + 2\Re \left(\sum_{k=1}^{N-1} z_k e^{-jk\omega} \right) \geq 0 \tag{46}$$

where

$$z_k \triangleq \sum_{i=1}^{N-k} Z_{i+k, i}, \quad 0 \leq k \leq N-1. \tag{47}$$

We use Theorem 3.2 of [36] (which is stated as Theorem 1 below) to obtain an SDP representation of

(46).

Theorem 1. *The trigonometric polynomial $\tilde{h}(\omega) = z_0 + 2\Re\left(\sum_{k=1}^{N-1} z_k e^{-jk\omega}\right)$ is non-negative for any $\omega \in [\omega_0 - \omega_1, \omega_0 + \omega_1]$ (with $0 < \omega_1 < \pi$) iff there exist an $N \times N$ Hermitian matrix $\mathbf{Z}_1 \succeq \mathbf{0}$ and an $(N-1) \times (N-1)$ Hermitian matrix $\mathbf{Z}_2 \succeq \mathbf{0}$ such that*

$$\mathbf{z} = \mathbf{F}_1^H\left(\text{diag}(\mathbf{F}_1\mathbf{Z}_1\mathbf{F}_1^H) + \mathbf{q} \odot \text{diag}(\mathbf{F}_2\mathbf{Z}_2\mathbf{F}_2^H)\right) \tag{48}$$

where $\mathbf{z} = [z_0 \; z_1 \; ... \; z_{N-1}]^T$, $\mathbf{q} = [q_0 \; q_1 \; ... \; q_{n-1}]^T$ with $q_k = \cos(2\pi k/n - \omega_0) - \cos(\omega_1)$, $\mathbf{F}_1 = [\mathbf{f}_0 \; ... \; \mathbf{f}_{N-1}]$ and $\mathbf{F}_2 = [\mathbf{f}_0 \; ... \; \mathbf{f}_{N-2}]$ in which $\mathbf{f}_k = [1 \; e^{-jk\theta} \; ... \; e^{-j(n-1)k\theta}]^T$ with $\theta = 2\pi/n$, and $n \geq 2N - 1$.

Note that the SDP representation of (46) can be derived by employing the above results with $n = 2N - 1$, $\omega_0 = (\omega_l + \omega_u)/2$, and $\omega_1 = \omega_0 - \omega_l$.

Next we obtain an LMI representation for the constraint (45). Let $\mathbf{G} = \text{Diag}([G_1 \; G_2 \; ... \; G_N]) = \sum_{m=1}^{N} \mathbf{g}_m \mathbf{g}_m^H$ (where $\mathbf{g}_m = \sqrt{G_m}\mathbf{e}_m$), and note that

$$\text{tr}\left\{(\mathbf{Z}^{-1} - \mathbf{C})^{-1}\mathbf{G}\right\} = \sum_{m=1}^{N}\left\{\mathbf{g}_m^H\mathbf{Z}\mathbf{g}_m + \mathbf{g}_m^H\mathbf{Z}\mathbf{B}(\mathbf{I} - \mathbf{B}^H\mathbf{Z}\mathbf{B})^{-1}\mathbf{B}^H\mathbf{Z}\mathbf{g}_m\right\}. \tag{49}$$

Similar to the derivation of CoRe in the average-sense code design, we consider the following LMI characterization:

$$\mathbf{g}_m^H\mathbf{Z}\mathbf{g}_m + \mathbf{g}_m^H\mathbf{Z}\mathbf{B}(\mathbf{I} - \mathbf{B}^H\mathbf{Z}\mathbf{B})^{-1}\mathbf{B}^H\mathbf{Z}\mathbf{g}_m \quad \leq \gamma_m \tag{50}$$

$$\Leftrightarrow \begin{bmatrix} \gamma_m - \mathbf{g}_m^H\mathbf{Z}\mathbf{g}_m & \mathbf{g}_m^H\mathbf{Z}\mathbf{B} \\ \mathbf{B}^H\mathbf{Z}\mathbf{g}_m & \mathbf{I} - \mathbf{B}^H\mathbf{Z}\mathbf{B} \end{bmatrix} \quad \succeq 0$$

where $\{\gamma_m\}$ are auxiliary variables. Therefore, the SDP related to the worst-case code design can be

expressed as[5]:

$$\text{CSDP:} \quad \max_{t,\mathbf{Z},\mathbf{Z}_1,\mathbf{Z}_2,\{\gamma_m\}_{m=1}^{N}} \{t\} \tag{51}$$

subject to

$$\mathbf{z} = t\mathbf{e}_1 + \mathbf{F}_1^H \left(\text{diag}(\mathbf{F}_1\mathbf{Z}_1\mathbf{F}_1^H) + \mathbf{q} \odot \text{diag}(\mathbf{F}_2\mathbf{Z}_2\mathbf{F}_2^H) \right),$$

$$\begin{bmatrix} \gamma_m - \mathbf{g}_m^H \mathbf{Z} \mathbf{g}_m & \mathbf{g}_m^H \mathbf{Z} \mathbf{B} \\ \mathbf{B}^H \mathbf{Z} \mathbf{g}_m & \mathbf{I} - \mathbf{B}^H \mathbf{Z} \mathbf{B} \end{bmatrix} \succeq \mathbf{0}, \quad \forall\, m,$$

$$\sum_{m=1}^{N} \gamma_m \leq e,$$

$$\mathbf{I} - \mathbf{B}^H \mathbf{Z} \mathbf{B} \succ \mathbf{0},$$

$$\mathbf{Z} \succ \mathbf{0}, \ \mathbf{Z}_1 \succeq \mathbf{0}, \ \mathbf{Z}_2 \succeq \mathbf{0}.$$

To synthesize the code matrix $\mathbf{A}$ from the CSDP solution $\mathbf{Z}$ of (51), we will consider a synthesis stage similar to that of the average-sense code design in sub-section III-A (observe that $(\mathbf{Z}^{-1} - \mathbf{C})^{-1} = \mathbf{X}$). The CoRe framework for obtaining optimized codes using the worst-case metric is summarized in Table III. Although solving (51) yields a global optimum of the CSDP, the further synthesis step leads to an approximate solution $\mathbf{A}$ of the original problem in (42). Therefore, the CSDP solution of (51) provides an upper bound on the possible values of the worst-case metric. Note that the results can be straightforwardly extended to the case in which Ω is a union of several intervals.

TABLE III
CoRe for Optimal Code Design Using the Worst-Case Metric

Step 1: Solve CSDP in (51) to obtain its global optimum $\mathbf{Z}$.
Step 2 *(The synthesis stage)*: Initialize the code vector $\mathbf{a}$ with a random vector in $\mathbb{C}^N$.
    Step 2-1: Compute $\mathbf{Q} = \mathbf{V}_2\mathbf{V}_1^H$ where $\mathbf{V}_1\mathbf{S}\mathbf{V}_2^H$ represents the SVD of $\mathbf{M}^{-1/2}\mathbf{A}(\mathbf{Z}^{-1} - \mathbf{C})^{-1/2}$.
    Step 2-2: Compute the code vector as

$$\mathbf{a} = \mathbf{G}\ \text{diag}\left((\mathbf{Z}^{-1} - \mathbf{C})^{-1/2}\mathbf{Q}^*\mathbf{M}^{-1/2} \right).$$

Step 2-3: Repeat steps 2-1 and 2-2 until a pre-defined stop criterion is satisfied, e.g. $\|\mathbf{a}^{(k+1)} - \mathbf{a}^{(k)}\| \leq \epsilon$ for some $\epsilon > 0$, where k denotes the iteration number.

---

[5]We have also included the constraint $\mathbf{I} - \mathbf{B}^H\mathbf{Z}\mathbf{B} \succ \mathbf{0}$ in the CSDP (51) to ensure a meaningful synthesis stage (see Remark 3 below).

Remark 3: The reader might observe the fact that the code synthesis stage is meaningful only if $\mathbf{Z} \prec \mathbf{C}^{-1}$, and hence might be willing to add such constraint to the constraint set of (51). To clarify this issue, note that using the matrix inversion lemma we have

$$(\mathbf{Z}^{-1} - \mathbf{C})^{-1} = \mathbf{Z} + \mathbf{Z}\mathbf{B}(\mathbf{I} - \mathbf{B}^H\mathbf{Z}\mathbf{B})^{-1}\mathbf{B}^H\mathbf{Z}. \tag{52}$$

As $\mathbf{Z}$ of (51) is a positive-definite matrix, and the constraint set in (51) implies $\mathbf{I} - \mathbf{B}^H\mathbf{Z}\mathbf{B} \succ \mathbf{0}$, we conclude from (52) that $\mathbf{Z}^{-1} - \mathbf{C} \succ \mathbf{0}$. Therefore, the constraint $\mathbf{Z} \prec \mathbf{C}^{-1}$ is already taken into account via the constraints in (51). Moreover, adding the constraint $\mathbf{Z} \prec \mathbf{C}^{-1}$ separately would limit our design to the case of a non-singular $\mathbf{C}$. ∎

V. CONSTRAINED CODE DESIGN

In order to use the power resources efficiently and to avoid non-linear effects at the transmitter, sequences with low PAR values are of practical interest in many applications [19] [37]. In this section, we consider code design via CoRe and CADCODE frameworks under an arbitrary PAR constraint, viz.

$$\text{PAR}(\mathbf{a}) = \frac{\max_m \{|a_m|^2\}}{\frac{1}{N}\|\mathbf{a}\|^2} \leq \zeta. \tag{53}$$

It is possible to synthesize low-PAR codes from the CSDP solution of the CoRe framework. To keep the paper concise, we only use the CoRe formulation in an average sense (note that for a worst-case scenario we have $(\mathbf{Z}^{-1} - \mathbf{C})^{-1} = \mathbf{X}$). In this case, the optimization problem (26) can be reformulated as

$$\min_{\mathbf{A},\mathbf{Q}} \quad \|\mathbf{X}^{1/2}\mathbf{Q} - \mathbf{A}^H\mathbf{M}^{-1/2}\|_F^2 \tag{54}$$

$$\text{subject to} \quad \mathbf{Q}\mathbf{Q}^H = \mathbf{I}$$

$$\text{PAR}(\mathbf{a}) \leq \zeta.$$

Therefore, for fixed $\mathbf{Q}$ we have the code synthesis problem:

$$\max_{\mathbf{a}} \quad \mathbf{a}^H(\mathbf{M}^{-1} \odot \mathbf{I})\mathbf{a} - 2\Re\left(\mathbf{b}^H\mathbf{a}\right) \tag{55}$$

$$\text{subject to} \quad \max_{m=0,\cdots,N-1} \{|a_m|^2\} \leq \zeta,$$

$$\|\mathbf{a}\|^2 = N.$$

On the other hand, the low-PAR code design using the CADCODE framework can be handled in a similar manner. The minimization of $g(\mathbf{Y}, \mathbf{A})$ in (35) w.r.t. a low-PAR code vector $\mathbf{a}$ can be accomplished using

the optimization problem

$$\min_{\mathbf{a}} \quad \mathbf{a}^H \left((\mathbf{Y}_2 \mathbf{Y}_2^H) \odot \mathbf{C}^T \right) \mathbf{a} + 2\Re(\mathbf{d}^H \mathbf{a}) \tag{56}$$

$$\text{subject to} \quad \max_{m=0,\cdots,N-1} \{|a_m|^2\} \leq \zeta,$$

$$\|\mathbf{a}\|^2 = N.$$

We note that both (55) and (56) are non-convex QCQPs with PAR constraint and known to be NP-hard in general [19]. In the following, we consider the formulation of (55) (without loss of generality). The optimization problem in (55) is equivalent to

$$\min_{\mathbf{a}} \quad \widetilde{\mathbf{a}}^H \mathbf{J} \, \widetilde{\mathbf{a}} \tag{57}$$

$$\text{subject to} \quad \max_{m=0,\cdots,N-1} \{|a_m|^2\} \leq \zeta,$$

$$\|\mathbf{a}\|^2 = N$$

where $\widetilde{\mathbf{a}} = [\mathbf{a} \quad 1]^T$, and

$$\mathbf{J} = \begin{bmatrix} \mathbf{M}^{-1} \odot \mathbf{I} & -\mathbf{b} \\ -\mathbf{b}^H & 0 \end{bmatrix}.$$

For any $\mu > \lambda_{max}(\mathbf{J})$ we can reformulate the latter problem as

$$\max_{\mathbf{a}} \quad \widetilde{\mathbf{a}}^H \mathbf{K} \, \widetilde{\mathbf{a}} \tag{58}$$

$$\text{subject to} \quad \max_{m=0,\cdots,N-1} \{|a_m|^2\} \leq \zeta,$$

$$\|\mathbf{a}\|^2 = N$$

with $\mathbf{K} = \mu \mathbf{I}_{N+1} - \mathbf{J}$. Interestingly, derivation of the power-method like iterations in [38] [39] can be extended to the case of PAR-constrained $\mathbf{a}$. As a result, the discussed iterations can be applied (after a small modification) to obtain a local optimum of (58). More precisely, the code vector $\mathbf{a}$ of the $(l+1)^{th}$ iteration (denoted by $\mathbf{a}^{(l+1)}$) can be obtained from the last estimate of $\mathbf{a}$, i.e. $\mathbf{a}^{(l)}$, via solving the optimization problem

$$\max_{\mathbf{a}^{(l+1)}} \quad \|\mathbf{a}^{(l+1)} - \widehat{\mathbf{a}}^{(l)}\| \tag{59}$$

$$\text{subject to} \quad \max_{m=0,\cdots,N-1} \{|a_m^{(l+1)}|^2\} \leq \zeta,$$

$$\|\mathbf{a}^{(l+1)}\|^2 = N$$

where $\widehat{\mathbf{a}}^{(l)}$ represents the vector containing the first N entries of $\mathbf{K}\,\widetilde{\mathbf{a}}^{(l)}$. The optimization problem (59) is a "nearest-vector" problem with PAR constraint. Such PAR constrained problems can be tackled using a recursive algorithm proposed in [40] that can be described briefly as follows: for cases in which the magnitudes of the entries of $\widehat{\mathbf{a}}^{(l)}$ are below $\sqrt{\zeta}$, one can easily observe that $\mathbf{a}^{(l+1)} = \sqrt{N}\widehat{\mathbf{a}}^{(l)}/\|\widehat{\mathbf{a}}^{(l)}\|$ is the solution. Otherwise, let $\widehat{a}_0$ denote the entry of $\widehat{\mathbf{a}}^{(l)}$ with maximum absolute value. Then the entry of $\mathbf{a}^{(l+1)}$ corresponding to $\widehat{a}_0$ is given by $\sqrt{\zeta}e^{j\arg(\widehat{a}_0)}$. Recursively, the other entries of $\mathbf{a}^{(l+1)}$ can be obtained solving the same type of "nearest-vector" problem but with the remaining energy i.e. $N - \zeta$.

Finally, we note that as a scaling does not affect the PAR metric (see (53)), the low-PAR codes obtained by CoRe or the CADCODE framework can be scaled to fit any desired level of energy. The steps of CoRe and CADCODE presented in Table I and Table II should be modified for designing low-PAR codes. More precisely, the optimization problems in (55) in step 2-2 of CoRe (average design) and (56) in step 2 of CADCODE are solved via the power method-like iterations provided above.

Remark 4 (unimodular code design): In case of unimodular code design, i.e. $\zeta = 1$, we have

$$\operatorname{tr}\left\{\mathbf{A}^H\mathbf{M}^{-1}\mathbf{A}\right\} = \mathbf{a}^H(\mathbf{M}^{-1}\odot\mathbf{I})\mathbf{a} \tag{60}$$
$$= N\operatorname{tr}\left\{\mathbf{M}^{-1}\odot\mathbf{I}\right\} = N\operatorname{tr}\left\{\mathbf{G}^{-1}\right\}$$

and hence the optimization problem in (55) is equivalent to:

$$\max_{\mathbf{a}} \quad \Re(\mathbf{b}^H\mathbf{a}) \tag{61}$$
$$\text{subject to} \quad |a_m| = 1, \ \ 0 \leq m \leq N - 1$$

where $\mathbf{b} = \operatorname{diag}(\mathbf{X}^{1/2}\mathbf{Q}^*\mathbf{M}^{-1/2})$. The maximizer $\mathbf{a}$ of (61) is simply given by $\mathbf{a} = \exp(j\arg(\mathbf{b}))$. As to the CADCODE framework, unimodular codes can alternatively be obtained by defining

$$\mathbf{R} \triangleq \begin{bmatrix} \theta\mathbf{I} & \mathbf{V}^H \\ \mathbf{V} & (\mathbf{A}^H\mathbf{M}^{-1}\mathbf{A})^{-1} + \mathbf{C} \end{bmatrix} \tag{62}$$

with sufficiently large θ (see Appendix C). Note that for $g(\mathbf{Y}, \mathbf{A}) = \operatorname{tr}\{\mathbf{Y}^H\mathbf{R}\mathbf{Y}\}$ with above $\mathbf{R}$, eqs. (34) and (38) hold true. Therefore, for fixed $\mathbf{Y}$ the minimization of $g(\mathbf{Y}, \mathbf{A})$ w.r.t. $\mathbf{A}$ can be simplified as the following homogeneous QCQP:

$$\min_{\mathbf{A}} \quad \operatorname{tr}\left\{\mathbf{Y}_2\mathbf{Y}_2^H\mathbf{A}^H\mathbf{M}\mathbf{A}\right\} \tag{63}$$
$$\text{subject to} \quad |a_m| = 1, \ \ 0 \leq m \leq N - 1$$

where $\mathbf{Y} = [\mathbf{Y}_{1\ \delta\times\delta}\ \ \mathbf{Y}_{2\ N\times\delta}]$. The unimodular quadratic programm in (63) is NP-hard in general and can be tackled via a technique similar to that of (58). ∎

VI. NUMERICAL EXAMPLES

Numerical results will be provided to examine the performance of the proposed methods. Several code design examples for the average metric and the worst-case metric in both constrained and unconstrained cases are included. In particular, we provide a comparison between the code designs in the average and worst-case scenarios using SNR defined in (9).

Throughout the numerical examples, we assume that the signal-independent interference can be modeled as a first-order auto-regressive process with parameters $\rho_{\text{int}} = 0.5$ and p_{int}, as well as a white noise at the receiver with the variance σ_n^2:

$$M_{m,n} = \sigma_n^2 \delta[m-n] + p_{\text{int}}\rho_{\text{int}}^{|m-n|}, \ 1 \le m, n \le N \tag{64}$$

with $\delta[m-n]$ being the discrete-time Kronecker delta function. Furthermore, for clutter we let

$$C_{m,n} = \sigma_c^2 \rho^{(m-n)^2}, \ 1 \le m, n \le N \tag{65}$$

with $\rho = 0.8$. Note that the model in (65) can be used for many natural clutter sources [41]. In this section, we consider $\sigma_c^2 = 1, \sigma_n^2 = 0.01$, and $p_{\text{int}} = 1$ unless otherwise explicitly stated. As to the unknown target Doppler shift, we assume ω is uniformly distributed over Ω. The CVX package has been used to solve the convex problems in the various approaches of this paper [42]. The extensions of the CoRe and CADCODE frameworks to the case of unimodular code design ($\zeta = 1$) are referred to as CoRe-U and CADCODE-U, respectively (for CoRe and CADCODE without suffix "U" we do not consider the PAR constraint).

A. Average design

Herein we consider an example of code design for a Doppler shift interval of $[\omega_l, \omega_u] = [-1, 1]$. We use the proposed algorithms (both CoRe and CADCODE frameworks) to design optimal codes of length $N = 16$. The results are shown in Fig. 1(a). The goodness of the resultant codes is investigated using two benchmarks: (i) the upper bound on the average metric obtained by solving the CSDP in (25), and (ii) the average metric corresponding to the uncoded system (using the transmit code $\mathbf{a} = \sqrt{\frac{e}{N}}\mathbf{1}$).

It can be observed from Fig. 1(a) that, as expected, a coded system employing CoRe, CoRe-U, CADCODE, or CADCODE-U outperforms the uncoded system. It is also practically observed that the

performance obtained by the randomly generated codes is similar to that of the all-one code used in the uncoded system. We also note that, compared to CoRe, the CADCODE framework leads to slightly larger values of the average metric. This behaviour can be explained noting that CADCODE presumably circumvents the optimality losses arising in the synthesis stage of CoRe. In other words, CADCODE directly converges to a stationary point of the design problem and there is no synthesis loss associated with the provided code; whereas, the obtained code via CoRe is associated with some synthesis loss. Moreover, Fig. 1(a) reveals that the quality of the codes obtained via constrained designs is very similar to that of unconstrained designs. However, there are minor degradations due to imposing the constraints. We also observe the saturation phenomenon in Fig. 1(a). More precisely, for sufficiently large values of the transmit energy (i.e. e), the increase in the average metric is negligible. Note that, the value of the average metric (for non-singular $\mathbf{C}$) asymptotically converges to:

$$\lim_{e \to \infty} \mathrm{tr}\left\{\left((\mathbf{A}^H\mathbf{M}^{-1}\mathbf{A})^{-1} + \mathbf{C}\right)^{-1}\mathbf{W}\right\} = \mathrm{tr}\{\mathbf{C}^{-1}\mathbf{W}\}. \tag{66}$$

Next we study the performance of the proposed algorithms w.r.t. the detection performance of the optimal detector (for unknown Doppler shift) stated in (11). To this end, we consider the target with $\sigma_T^2 = 10$, transmit energy $e = 10$, and use 100000 sets of random generated data to simulate receiver operating characteristic (ROC). The optimal detector in (11) is implemented by numerically evaluating the associated integral. ROCs corresponding to CoRe and CADCODE algorithms (constrained and unconstrained case) as well as to the uncoded system are depicted in Fig. 1(b). As expected, the detection performance obtained by devised methods outperforms that of the uncoded system. Minor differences can be observed between ROCs associated with various algorithms. The practical implementation of the optimal detector in (11) might be hard. Therefore, we also consider a conventional GLR detector that well approximates the behavior of the optimal detector ([43] [26]):

$$\max_{\omega \in \Omega} \frac{|\mathbf{r}^H \left(\mathbf{M} + \mathbf{ACA}^H\right)^{-1} (\mathbf{a} \odot \mathbf{p})|^2}{(\mathbf{a} \odot \mathbf{p})^H \left(\mathbf{M} + \mathbf{ACA}^H\right)^{-1} (\mathbf{a} \odot \mathbf{p})} \underset{\mathrm{H_1}}{\overset{\mathrm{H_0}}{\lessgtr}} \eta'' \tag{67}$$

In practical situations, a discrete set of target Doppler shifts in Ω is considered in lieu of Ω for the maximization. Fig. 1(c), plots the detection performance of the above detector for the coded and uncoded systems (employing 50 points in the Ω for the maximization). As expected, there exist minor degradations in the detection performance of the systems as compared with the performance of the optimal detector shown in Fig. 1(b). This figure corresponds to CADCODE but similar performances were observed for the other proposed methods.

The effect of the code length N on the value of the average metric is illustrated in Fig. 2 for a fixed transmit energy $e = 10$. It can be seen that as N grows large, the quality of the proposed coding schemes improves substantially (compared to the uncoded system). This is due to the fact that for a large N the code design problem has more degrees of freedom. It can also be observed in Fig. 2 that for any fixed length, CoRe and CADCODE provide similar results.

The detection performance of the system depends on the energy of the clutter and interference. To investigate the effects of the aforementioned parameters on the system performance, we define the clutter-to-noise ratio (CNR) and the interference-to-noise ratio (INR):

$$CNR = \frac{\sigma_c^2 \, e}{\sigma_n^2}$$
$$INR = \frac{p_{\text{int}}}{\sigma_n^2}$$

To measure the performance improvement in different scenarios, we consider the improvement of the average metric (13) (i.e., $\text{metric}^{\text{imp}}$) and the relative increment of the detection probability associated with the optimal detector (11) (i.e., P_d^{inc}) w.r.t. the uncoded system:

$$\text{metric}^{\text{imp}} = \frac{\text{average metric}^{coded}}{\text{average metric}^{uncoded}}$$
$$P_d^{\text{inc}} = P_d^{coded} - P_d^{uncoded}$$

The values of $\text{metric}^{\text{imp}}$ and P_d^{inc} for different CNRs have been shown in Table IV. The reported values are associated with $e = 5$, INR $= 20$ dB, $\sigma_T^2 = 5$ and are obtained via changing σ_c^2. Note that these values correspond to CADCODE but similar behaviors were observed for the other methods. As to the P_d^{inc}, the ROC of the optimal detector (11) is considered for $P_{fa} = 10^{-3}$. It is observed that P_d^{inc} is an increasing function of $\text{metric}^{\text{imp}}$. This can be explained via considering the mathematical reasoning for using the average metric (see section III). Furthermore, as expected, increasing the energy of clutter leads to the decreasing of $\text{metric}^{\text{imp}}$ (and so P_d^{inc}). Indeed, for sufficiently large values of CNR, the term $\mathbf{A}^{-1}\mathbf{M}\mathbf{A}^{-H}$ can be neglected as compared with $\mathbf{C}$ in (13); therefore, the effect of the code matrix $\mathbf{A}$ on the detection performance is minor (see the similar discussion on the saturation phenomenon).

Next we perform a similar analysis to probe the detection performance of the system for different values of INR. Herein we consider $e = 5$, CNR $= 20$ dB, $\sigma_T^2 = 5$ and report the values of $\text{metric}^{\text{imp}}$ and P_d^{inc} associated with CADCODE in Table V (by changing p_{int}). It is observed that in low INRs, the performance improvement is minor; this can be explained by noting the fact that such situations refer to clutter-limited cases. By increasing the energy of interference (i.e., going from clutter-limited conditions

CNR	10 dB	15 dB	20 dB	25 dB	30 dB
metric$^{\text{imp}}$	6.65 dB	6.1 dB	5.3 dB	3.9 dB	2.2 dB
P_d^{inc}	0.32	0.31	0.28	0.23	0.15

to interference-limited conditions), the performance improvement increases. This observation is related to the fact that the the proposed methods have better ability for reducing the effects of the signal-independent interference (as compared with the signal-dependent clutter). Also, it is expected that for large enough values of INR, the detection probabilities of both coded and uncoded systems significantly reduce; hence P_d^{inc} becomes small.

TABLE V
THE VALUES OF metric$^{\text{imp}}$ AND P_d^{inc} FOR DIFFERENT INRs (CADCODE).

INR	10 dB	15 dB	20 dB	25 dB	30 dB
metric$^{\text{imp}}$	2.2 dB	3.9 dB	5.3 dB	6.2 dB	6.6 dB
P_d^{inc}	0.08	0.13	0.28	0.42	0.42

B. Worst-case design

We consider a worst-case design example with code length $N = 16$, transmit energy $e = 10$, and the Doppler shift interval $\Omega = [-1.5, -0.5] \cup [0.5, 1.5]$. The assessment of the codes in the worst-case design is performed using: (i) the CSDP solution of (51) which leads to an upper bound on the worst-case metric, and (ii) the worst-case metric values associated with the uncoded system.

The SNR corresponding to i) and ii) above and to the coded system using CoRe as well as CoRe-U are shown in Fig. 3(a) versus the target Doppler shift ω for $\sigma_T^2 = 1$. The optimized CoRe and CoRe-U codes outperform the uncoded system significantly. Moreover, a minor difference between the lowest SNR of the optimized codes can be observed. Note that near $\omega = 0$, all the curves show worse values as compared to other values of ω. This is due to the overlapping of the target and clutter in the frequency domain. The detection probability can be used to obtain further insights into the behaviour of the worst-case metric for code optimization. We consider the worst-case detection probabilities w.r.t. the Doppler shift of the

target. Let $\tilde{\omega}$ denote the Doppler shift corresponding to the smallest achievable performance metric w.r.t ω, viz.

$$\tilde{\omega} = \underset{\omega_l \leq \omega \leq \omega_u}{\arg\min} \ \mathrm{tr}\left\{\left((\mathbf{A}^H\mathbf{M}^{-1}\mathbf{A})^{-1} + \mathbf{C}\right)^{-1}\mathbf{pp}^H\right\}. \tag{68}$$

The values of $\tilde{\omega}$ were computed via the Newton method. The worst-case detection probability is calculated via results of [19] as

$$P_{d,worst} = \exp\left(\frac{\log(P_{fa})}{1 + \tilde{\lambda}}\right) \tag{69}$$

where P_{fa} denotes probability of false alarm and $\tilde{\lambda}$ is the value of λ for $\tilde{\omega}$. Using the obtained $\tilde{\omega}$ and (69), Fig. 3(b) shows the worst-case detection probabilities for the CSDP solution and the CoRe code versus target strength σ_T^2 for $P_{fa} = 10^{-6}$. Using CoRe and CoRe-U, a substantial improvement of $P_{d,worst}$ is evident compared to the uncoded system. Due to the unimodularity constraint, CoRe-U yields a slightly lower worst-case detection probability compared to CoRe.

C. Comparison of the Average and Worst-Case Designs

The average and worst-case metrics are independent of the target Doppler shift; however, one can use the SNR (for various ω) to compare the average and the worst-case designs. To compare the two designs, we consider a code length of $N = 16$, transmit energy $e = 10$, $\sigma_T^2 = 1$, and two different Doppler shift intervals $[-2, -1] \cup [1, 2]$ and $[-2, -0.5] \cup [0.5, 2]$. Fig. 4(a)-(b) plot the SNRs corresponding to the CSDP solution in (25), the code obtained by CoRe for the average design, the CSDP solution in (51) and the code obtained by CoRe for the worst-case design. These sub-figures also show the SNR corresponding to the case in which the target Doppler shift is known. Note that for the aforementioned case, the optimized code is obtained via the maximization of (12) for each Doppler and hence various target Doppler shifts lead to various optimal codes. The SNR associated with the known Doppler case always has the largest values compared with other feasible codes. However, the CSDP solution (51) possesses larger minimum SNR values when compared to other curves; but the optimized code corresponding to the CSDP solution (51) is associated with a certain synthesis loss that leads to slightly lower minimum value as compared to the known Doppler case. The codes obtained via the worst-case design provide better minimum SNR values whereas the codes obtained via the average design possess larger average SNR values. Furthermore, there exist nulls near $\omega = 0$ due to the overlapping of the target and clutter spectra. In addition, the CSDP solution of the worst-case design can be considered to be rather "conservative" when compared to that of the average design. Herein we remark on the fact that the worst-case design

does not require the p.d.f of the target Doppler shift on the desired interval Ω; whereas, the average design depends on the aforementioned p.d.f. Fig. 4(c)-(d) depict the detection probabilities corresponding to sub-figures Fig. 4(a)-(b). The values of detection probability are obtained via considering (69) with $P_{fa} = 10^{-6}$ and $\sigma_T^2 = 10$. Observations similar to those about sub-figures Fig. 4(a)-(b) can be made from these sub-figures as well.

VII. CONCLUDING REMARKS

The problem of radar code design for moving target detection in the presence of clutter was considered. Several algorithms were proposed using two novel frameworks for unconstrained or constrained code design in such scenarios. The main results can be summarized as follows:

- A new discrete-time formulation was introduced in (4) for moving target detection using pulsed-radars in the presence of clutter (considering motions of the clutter scatterers). The optimal detectors for both known Doppler shift and unknown Doppler shifts are presented. To handle the unknown Doppler shift of the target, the code design problem was considered using both average and worst-case performance metrics of the optimal detector for known Doppler shifts. The connection between the considered metrics and the detection performance are addressed.

- The Convexification via Reparametrization (CoRe) framework was proposed to deal with the highly non-convex design problems. CoRe is based on a relaxation (reparametrization) of the metric optimization problems followed by a synthesis stage. The CoRe framework was used to develop two separate algorithms for obtaining optimal codes in both average and worst-case designs.

- The CoRe framework is based on a core SDP (called CSDP) which can be solved efficiently (in polynomial-time). The CSDP solution of CoRe was used to synthesize the optimal codes w.r.t. the original design problem. The code synthesis was accomplished using a cyclic optimization of a similarity criterion. The CSDP solution provides an upper bound on the average metric in different design scenarios.

- A Cyclic Algorithm for Direct COde DEsign, namely the CADCODE framework, was suggested to tackle the average code design problem directly. In CADCODE, the code design objective function is iteratively minimized via a cyclic minimization of an auxiliary function of the code matrix. The convergence of CADCODE was studied. It was shown that each step of CADCODE can be performed either using the available analytical solutions or solving a convex QCQP.

- The design problems when PAR constrained codes are of interest were also considered. The derivations of CoRe and CADCODE were extended to tackle such constrained problems.

- Several numerical examples were provided to show the potential of the proposed algorithms. It was observed that the codes obtained by CADCODE generally have slightly larger metrics in comparison to those obtained using the synthesis stage of CoRe. The CSDP solution of the worst-case design appears to be rather "conservative" when compared to that of the average design.

Finally we note that, in this paper, the covariance matrices of the clutter and interference assumed to be a priori known. However, in practice, the matrices are not exactly known and need to be estimated. The code design problem considering uncertainty of the prior knowledge about statistics of clutter and interference can be an interesting topic for future research.

APPENDIX A

DERIVATION OF THE DISCRETE-TIME MODEL

It follows from (1) and (2) that the nth lag of the receiver filter output sampled at $t = nT_{PRI} + \tau$ can be written as

$$
\begin{aligned}
r_n &= \left. (r(t)e^{-j\omega_c t}) \star \phi^*(-t) \right|_{t=nT_{PRI}+\tau} \\
&= \int_{-\infty}^{+\infty} r(x)e^{-j\omega_c x} \phi^*(x - nT_{PRI} - \tau) dx \\
&= \int_{-\infty}^{+\infty} \alpha_t e^{-j(\omega_c+\nu)\tau} \sum_{m=0}^{N-1} a_m \phi(x - mT_{PRI} - \tau) e^{j\nu x} \phi^*(x - nT_{PRI} - \tau) dx \\
&\quad + \int_{-\infty}^{+\infty} \sum_{k=1}^{N_{ct}} \sum_{l=1}^{N_{cd}} \sum_{m=0}^{N-1} e^{-j(\omega_c+\omega_l)\tau_k} \rho_{kl} a_m \phi(x - mT_{PRI} - \tau_k) e^{j\omega_l x} \phi^*(x - nT_{PRI} - \tau) dx \\
&\quad + \int_{-\infty}^{+\infty} w(x)e^{-j\omega_c x} \phi^*(x - nT_{PRI} - \tau) dx
\end{aligned}
\tag{70}
$$

where $\star$ denotes the convolution operator. For the first term at the right-hand side (RHS) of (70) we have that

$$
\begin{aligned}
& \alpha_t \sum_{m=0}^{N-1} a_m e^{-j\omega_c \tau} e^{j\nu m T_{PRI}} \\
& \times \int_{-\infty}^{+\infty} \phi(x - mT_{PRI} - \tau) \phi^*(x - nT_{PRI} - \tau) e^{j\nu(x - mT_{PRI}-\tau)} dx \\
&= \alpha e^{jn\omega} \sum_{m=0}^{N-1} a_m \Psi_{\mathrm{m,n}}(0, \nu)
\end{aligned}
\tag{71}
$$

where $\alpha \triangleq \alpha_t e^{-j\omega_c\tau}$, $\omega \triangleq \nu T_{PRI}$, and $\Psi_{\mathrm{m,n}}(t_d, \omega_d)$ is the cross-ambiguity function of $\phi(t - mT_{PRI})$ and $\phi(t - nT_{PRI})$ at $t_d = 0$ and Doppler shift ω_d, which is generally defined as

$$\Psi_{\mathrm{m,n}}(t_d, \omega_d) = \int_{-\infty}^{+\infty} \phi(x - mT_{PRI})\phi^*(x - nT_{PRI} - t_d)e^{j\omega_d(x - mT_{PRI})}dx. \tag{72}$$

Note that $\phi(t - mT_{PRI})$ and $\phi(t - nT_{PRI})$ are non-overlapping for any $n \neq m$. As $\Psi_{n,n}(.,.)$ is not dependent on n, we exploit the notation brevity $\Psi(.,.) = \Psi_{n,n}(.,.)$ and further assume $\Psi(0, \nu) \approx 1$ (this assumption implies the Doppler tolerable property [41] for the basic pulse $\phi(.)$ and has also been considered in several other publications, e.g., [19] [22] and references therein). Therefore, (71) becomes

$$\alpha a_n e^{jn\omega}\Psi(0, \nu) \tag{73}$$

The second term at the RHS of (70) can be rewritten as

$$\sum_{k=1}^{N_{ct}} \sum_{l=1}^{N_{cd}} \rho_{kl} e^{-j(\omega_c + \omega_l)\tau_k} \sum_{m=0}^{N-1} a_m \tag{74}$$

$$\times \int_{-\infty}^{+\infty} \phi(x - mT_{PRI} - \tau_k)e^{j\omega_l x}\phi^*(x - nT_{PRI} - \tau)dx$$

$$= \sum_{k=1}^{N_{ct}} \sum_{l=1}^{N_{cd}} \rho_{kl} e^{-j\omega_c\tau_k} \sum_{m=0}^{N-1} a_m e^{j\omega_l mT_{PRI}} \Psi_{\mathrm{m,n}}(\tau - \tau_k, \omega_l)$$

For unambiguous-range clutter scatterers we have $|\tau - \tau_k| < T_{PRI} - \tau_p$ and hence it is observed that $\phi(x - mT_{PRI} - \tau_k)$ and $\phi^*(x - nT_{PRI} - \tau)$ are non-overlapping for $n \neq m$. Hence for any $n \neq m$ we have that $\Psi_{\mathrm{m,n}}(\tau - \tau_k, \omega_l) = 0$ and as a result, (74) can be simplified as

$$a_n \underbrace{\left(\sum_{k=1}^{N_{ct}} \sum_{l=1}^{N_{cd}} \rho_{kl} e^{-j\omega_c\tau_k} e^{jn\omega_l T_{PRI}} \Psi(\tau - \tau_k, \omega_l) \right)}_{c_n} \tag{75}$$

$$= a_n c_n$$

Finally, we denote the last term at the RHS of (70) by w_n to obtain the discrete-time signal model as

$$\mathbf{r} = \alpha\mathbf{a} \odot \mathbf{p} + \mathbf{a} \odot \mathbf{c} + \mathbf{w} \tag{76}$$

where $\mathbf{r} \triangleq [r_0 \ r_1 \ \dots \ r_{N-1}]^T$, $\mathbf{p} \triangleq [1 \ e^{j\omega} \ \dots \ e^{j(N-1)\omega}]^T$, and $\mathbf{w} \triangleq [w_0 \ w_1 \ \dots \ w_{N-1}]^T$.

The covariance matrices of Gaussian random vectors $\mathbf{w}$ and $\mathbf{c}$ are required for the proposed code

design algorithms. Let

$$E\left\{\mathbf{w}\mathbf{w}^H\right\} \triangleq \mathbf{M}, \quad E\left\{\mathbf{c}\mathbf{c}^H\right\} \triangleq \mathbf{C}. \tag{77}$$

To compute the entries of $\mathbf{M}$ one can write

$$
\begin{aligned}
M_{m,n} &= E\{w_m w_n^*\} \\
&= \int_{-\infty}^{+\infty} \int_{-\infty}^{+\infty} E\{w(x)w^*(y)\}e^{-j\omega_c(x-y)} \\
&\quad \times \phi^*(x - mT_{PRI} - \tau)\phi(y - nT_{PRI} - \tau) \, dxdy \\
&= \int_{-\infty}^{+\infty} \int_{-\infty}^{+\infty} R_w(x,y)e^{-j\omega_c(x-y)} \\
&\quad \times \phi^*(x - mT_{PRI} - \tau)\phi(y - nT_{PRI} - \tau) \, dxdy
\end{aligned}
\tag{78}
$$

where $R_w(x,y)$ is the statistical auto-correlation function of the random process[6] $w(t)$. In particular, it is interesting to derive the entries of $\mathbf{C}$ as it provides useful insights into the importance of the ambiguity function of $\phi(.)$ as well as the other parameters that form $\mathbf{C}$. The entries of $\mathbf{C}$ can be computed as

$$
\begin{aligned}
C_{m,n} &= E\{c_m c_n^*\} \\
&= \sum_k \sum_l \sum_p \sum_q E\{\rho_{kl}\rho_{pq}^*\} E\{\left(e^{-j\omega_c\tau_k}e^{jm\omega_l T_{PRI}}\Psi(|\tau - \tau_k|, \omega_l)\right) \\
&\quad \times \left(e^{j\omega_c\tau_p}e^{-jn\omega_q T_{PRI}}\Psi^*(|\tau - \tau_p|, \omega_q)\right)\} \\
&= \sum_k \sum_l E\{|\rho_{kl}|^2\} E\{|\Psi(|\tau - \tau_k|, \omega_l)|^2 e^{j(m-n)\omega_l T_{PRI}}\}
\end{aligned}
\tag{79}
$$

where $E\{\rho_{kl}\}$ is assumed to be zero (without loss of generality). It is worth noting that $C_{m,n}$ is dependent on the variances of $\{\rho_{kl}\}$, the ambiguity function of $\phi(.)$ (i.e. $\Psi(.,.)$), as well as the statistical distributions of τ_k and ω_l .

APPENDIX B

TIGHTNESS ASSESSMENT OF THE LOWER BOUND $\mathcal{J}_{LB}$ ON THE J-DIVERGENCE

We define the following relative error to measure the tightness of the lower bound $\mathcal{J}_{LB}$ on the J-divergence:

$$\mathcal{E} \triangleq \frac{\mathcal{J} - \mathcal{J}_{LB}}{\mathcal{J}_{LB}}. \tag{80}$$

---

[6]Note that in the case of white noise, $M_{m,n}$ is zero for $m \neq n$ and $M_{n,n}$ is equal to the variance of the noise.

Let $\lambda_0 = \mathrm{E}\{\lambda\}$. Note that using (17), we have

$$\mathcal{J} = \mathrm{E}\left\{\lambda - 1 + \frac{1}{\lambda + 1}\right\} \tag{81}$$

and hence, the numerator of the relative error $\mathcal{E}$ can be simplified as:

$$
\begin{aligned}
\mathcal{J} - \mathcal{J}_{LB} &= \mathrm{E}\left\{\lambda - 1 + \frac{1}{\lambda + 1}\right\} - \left\{\lambda_0 - 1 + \frac{1}{\lambda_0 + 1}\right\} \\
&= \mathrm{E}\left\{\frac{1}{1 + \lambda}\right\} - \frac{1}{1 + \lambda_0}.
\end{aligned}
\tag{82}
$$

Note that there exists $\lambda_1 \geq 0$ for which $\lambda \geq \lambda_1$, for all ω. Therefore, we have $\mathrm{E}\left\{\frac{1}{1+\lambda}\right\} \leq \frac{1}{1+\lambda_1}$. Consequently, $\mathcal{E}$ can be upper bounded as:

$$\mathcal{E} \leq \frac{\lambda_0 - \lambda_1}{\lambda_0{}^2(1 + \lambda_1)} \leq \frac{1}{\lambda_0}. \tag{83}$$

The above analysis shows that for *sufficiently large* values of λ_0 the value of relative error $\mathcal{E}$ approaches zero. Hereafter, a numerical study of the tightness of the $\mathcal{J}_{LB}$ is provided. We first evaluate the relative error $\mathcal{E}$ for various intervals of ω. We consider $e = 16$, $\sigma_T^2 = 1$, and other parameters as those of Section VI. The value of the J-divergence is calculated by numerically evaluating the integral. Fig. 5(a) depicts two dimensional curve of the average of the $\mathcal{E}$ for 1000 random code vectors $\mathbf{a}$ versus ω' and ω''. Each point of the curve is associated with the Doppler shift interval $[\min(\omega', \omega''), \max(\omega', \omega'')]$. It is observed that the average $\mathcal{E}$ is significantly small. Moreover, as expected, average $\mathcal{E}$ is zero when $\omega' = \omega''$ (which corresponds to known Doppler shift equal to ω'). Next we investigate the behavior of the relative error with respect to the transmit energy e and target strength σ_T^2. The results are illustrated in Fig. 5(b) by considering 1000 random code vectors $\mathbf{a}$ and $\Omega = [-.75, 1.95]$ (corresponds to a peak of $\mathcal{E}$ in Fig. 5(a)). Small values of the average relative error can be seen in the figure. Furthermore, by increasing e or σ^2, the average $\mathcal{E}$ decreases. This observation is also compatible with the behavior of the $\mathcal{E}$ upper bound in (83).

APPENDIX C
DERIVATION OF THE VARIABLE θ

We note that θ should be sufficiently large such that Θ in (32) becomes positive definite. Particularly, θ should satisfy the matrix inequality

$$\theta\mathbf{I} - \mathbf{V}^H(\mathbf{A}^{-1}\mathbf{M}\mathbf{A}^{-H} + \mathbf{C})^{-1}\mathbf{V} \succ \mathbf{0} \tag{84}$$

or equivalently $\theta > \lambda_{max}\left(\mathbf{V}^H(\mathbf{A}^{-1}\mathbf{M}\mathbf{A}^{-H} + \mathbf{C})^{-1}\mathbf{V}\right)$. Note that

$$\lambda_{max}\left(\mathbf{V}^H(\mathbf{A}^{-1}\mathbf{M}\mathbf{A}^{-H} + \mathbf{C})^{-1}\mathbf{V}\right) \leq \lambda_{max}\left((\mathbf{A}^{-1}\mathbf{M}\mathbf{A}^{-H} + \mathbf{C})^{-1}\right)\lambda_{max}(\mathbf{W}). \tag{85}$$

Furthermore, one can verify that

$$\begin{aligned}
\lambda_{min}(\mathbf{A}^{-1}\mathbf{M}\mathbf{A}^{-H}) &= \min_{\|\mathbf{x}\|=1}\left((\mathbf{A}^{-H}\mathbf{x})^H\mathbf{M}(\mathbf{A}^{-H}\mathbf{x})\right) \tag{86} \\
&\geq \left(\min_m\{|a_m|^{-1}\}\right)^2\left(\min_{\|\mathbf{x}\|=1}\mathbf{x}^H\mathbf{M}\mathbf{x}\right) \\
&\geq \frac{1}{e}\lambda_{min}(\mathbf{M})
\end{aligned}$$

which implies

$$\begin{aligned}
\lambda_{min}(\mathbf{A}^{-1}\mathbf{M}\mathbf{A}^{-H} + \mathbf{C}) &\geq \lambda_{min}(\mathbf{A}^{-1}\mathbf{M}\mathbf{A}^{-H}) + \lambda_{min}(\mathbf{C}) \tag{87} \\
&\geq \frac{1}{e}\lambda_{min}(\mathbf{M}) + \lambda_{min}(\mathbf{C}).
\end{aligned}$$

As a result, setting

$$\theta = \frac{\lambda_{max}(\mathbf{W})}{\frac{1}{e}\lambda_{min}(\mathbf{M}) + \lambda_{min}(\mathbf{C})} \tag{88}$$

ensures $\Theta \succ \mathbf{0}$.

In the case of unimodular code design, we have that $|a_m| = 1$ (for all m). Therefore, in order to guarantee the positive definiteness of $\mathbf{R}$ in (62), it is sufficient to set

$$\theta = \frac{\lambda_{max}(\mathbf{W})}{\lambda_{min}(\mathbf{M}) + \lambda_{min}(\mathbf{C})}. \tag{89}$$

APPENDIX D

SOLUTION TO THE QCQP IN (37)

The convex QCQP in (37) can be solved using the Lagrange multiplier method . Let

$$h(\mathbf{a}, \mu) = \mathbf{a}^H\left(\mathbf{Y}_2\mathbf{Y}_2^H \odot \mathbf{C}^T\right)\mathbf{a} + 2\Re\left(\mathbf{d}^H\mathbf{a}\right) + \mu(\mathbf{a}^H\mathbf{a} - e) \tag{90}$$

represent the Lagrangian function with μ being the non-negative Lagrange multiplier associated with the energy constraint (such that $(\mathbf{Y}_2\mathbf{Y}_2^H) \odot \mathbf{C}^T + \mu\mathbf{I} \succ \mathbf{0}$). For fixed μ, the unconstrained minimizer $\mathbf{a}$ of $h(\mathbf{a}, \mu)$ is given by

$$\mathbf{a}_\mu = -(\mathbf{Y}_2\mathbf{Y}_2^H \odot \mathbf{C}^T + \mu\mathbf{I})^{-1}\mathbf{d}. \tag{91}$$

It is straightforward to derive that

$$h(\mathbf{a}_\mu, \mu) = -\mathbf{d}^H(\mathbf{Y}_2\mathbf{Y}_2^H \odot \mathbf{C}^T + \mu\mathbf{I})^{-1}\mathbf{d} - \mu e \tag{92}$$

The $h(\mathbf{a}_\mu, \mu)$ is a concave function w.r.t. $\mu \geq 0$ and hence the maximizer μ of (92) is immediate by imposing the criterion $\frac{\partial}{\partial \mu}h(\mathbf{a}_\mu, \mu) = 0$ which implies

$$\mathbf{d}^H(\mathbf{Y}_2\mathbf{Y}_2^H \odot \mathbf{C}^T + \mu\mathbf{I})^{-2}\mathbf{d} = e. \tag{93}$$

Moreover, note that

$$\frac{\partial}{\partial \mu}\left(\mathbf{d}^H(\mathbf{Y}_2\mathbf{Y}_2^H \odot \mathbf{C}^T + \mu\mathbf{I})^{-2}\mathbf{d}\right) = -2\mathbf{d}^H(\mathbf{Y}_2\mathbf{Y}_2^H \odot \mathbf{C}^T + \mu\mathbf{I})^{-3}\mathbf{d} < 0. \tag{94}$$

Therefore, the left hand side of (93) is a monotonically decreasing function of μ and hence the solution μ of (93) can be obtained efficiently via, for example, the Newton method. Once (93) is solved, the optimum $\mathbf{a}$ is calculated using (91).

REFERENCES

[1] W. D. Rummler, "A technique for improving the clutter performance of coherent pulse trains," *IEEE Trans. Aerosp. Electron. Syst.*, vol. 3, pp. 898–906, Nov. 1967.

[2] D. F. Delong and E. M. Hofstteter, "On the design of optimum radar waveforms for clutter rejection," *IEEE Trans. Inf. Theory*, vol. 13, pp. 454–463, Jul. 1967.

[3] ——, "The design of clutter-resistant radar waveforms with limited dynamic range," *IEEE Trans. Inf. Theory*, vol. 15, pp. 376–385, May 1969.

[4] L. J. Spafford, "Optimum radar signal processing in clutter," *IEEE Trans. Inf. Theory*, vol. 14, pp. 734–743, Sep. 1968.

[5] A. V. Balakrishnan, "Signal design for a class of clutter channels," *IEEE Trans. Inf. Theory*, vol. 14, pp. 170–173, Jan. 1968.

[6] S. M. Kay, "Optimal signal design for detection of Gaussian point targets in stationary Gaussian clutter/reverberation," *IEEE J. Sel. Topics Signal Process.*, vol. 1, pp. 31–41, Jun. 2007.

[7] P. Stoica, H. He, and J. Li, "Optimization of the receive filter and transmit sequence for active sensing," *IEEE Trans. Signal Process.*, vol. 60, no. 4, pp. 1730 –1740, Apr. 2012.

[8] A. Aubry, A. De Maio, M. Piezzo, A. Farina, and M. Wicks, "Cognitive design of the receive filter and transmitted phase code in reverberating environment," *IET Journal on Radar, Sonar, and Navigation*, vol. 6, no. 9, pp. 822–833, 2012.

[9] A. Aubry, A. De Maio, B. Jiang, and S. Zhang, "Ambiguity function shaping for cognitive radar via complex quartic optimization," *IEEE Trans. Signal Process.*, vol. 61, pp. 5603–5619, 2013.

[10] R. A. Romero, J. Bae, and N. A. Goodman, "Theory and application of SNR and mutual information matched illumination waveforms," *IEEE Trans. Aerosp. Electron. Syst.*, vol. 47, pp. 912–927, Apr. 2011.

[11] B. Friedlander, "Waveform design for MIMO radars," *IEEE Trans. Aerosp. Electron. Syst.*, vol. 43, pp. 1227–1238, Jul. 2007.

[12] C. Y. Chen and P. P. Vaidyanathan, "MIMO radar waveform optimization with prior information of the extended target and clutter," *IEEE Trans. Signal Process.*, vol. 57, pp. 3533–3544, Sep. 2009.

[13] T. Naghibi and F. Behnia, "MIMO radar waveform design in the presence of clutter," *IEEE Trans. Aerosp. Electron. Syst.*, vol. 47, pp. 770–781, Apr. 2011.

[14] R. S. Blum and Y. Yang, "MIMO radar waveform design based on mutual information and minimum mean-square error estimation," *IEEE Trans. Aerosp. Electron. Syst.*, vol. 43, pp. 330–343, Jan. 2007.

[15] B. Tang, J. Tang, and Y. Peng, "MIMO radar waveform design in colored noise based on information theory," *IEEE Trans. Signal Process.*, vol. 58, pp. 4684–4697, Sep. 2010.

[16] X. Song, P. Willett, S. Zhou, and P. Luh, "The MIMO radar and jammer games," *IEEE Trans. Signal Process.*, vol. 60, no. 2, pp. 687–699, Feb. 2012.

[17] A. De Maio, M. Lops, and L. Venturino, "Diversity integration trade-off in MIMO detection," *IEEE Trans. Signal Process.*, vol. 56, pp. 5051–5061, Oct. 2008.

[18] A. De Maio, Y. Huang, and M. Piezzo, "A Doppler robust max-min approach to radar code design," *IEEE Trans. Signal Process.*, vol. 58, pp. 4943–4947, Sep. 2010.

[19] A. De Maio, Y. Huang, M. Piezzo, S. Zhang, and A. Farina, "Design of optimized radar codes with a peak to average power ratio constraint," *IEEE Trans. Signal Process.*, vol. 59, pp. 2683–2697, Jun. 2011.

[20] H. L. Van Trees, "Optimum signal design and processing for reverberation-limited environments," *IEEE Transactions on Military Electronics*, vol. 9, no. 3, pp. 212–229, 1965.

[21] J. Li and P. Stoica, *MIMO Radar Signal Processing*, 1st ed. Wiley, 2008.

[22] A. Aubry, A. De Maio, A. Farina, and M. Wicks, "Knowledge-aided (potentially cognitive) transmit signal and receive filter design in signal-dependent clutter," *IEEE Trans. Aerosp. Electron. Syst.*, vol. 49, pp. 93–117, Jan. 2013.

[23] S. Haykin, "Cognitive radars," *IEEE Signal Process. Mag.*, vol. 23, no. 1, pp. 30–40, Jan. 2006.

[24] S. M. Kay, *Fundamentals of Statistical Signal Processing-Volume II: Detection Theory*, 1st ed. New Jersey: Prentice Hall, 1998.

[25] M. M. Naghsh, M. Soltanalian, P. Stoica, and M. Modarres-Hashemi, "Radar code optimization for moving target detection," in *21st European Signal Processing Conference*, Marrakech, Morocco, 2013.

[26] P. Stoica, J. Li, and M. Xue, "Transmit codes and receive filters for radar," *IEEE Signal Process. Mag.*, vol. 25, no. 6, pp. 94 –109, Nov. 2008.

[27] M. M. Naghsh, M. Modarres-Hashemi, S. ShahbazPanahi, M. Soltanalian, and P. Stoica, "Unified optimization framework for multi-static radar code design using information-theoretic criteria," *IEEE Trans. Signal Process.*, vol. 61, pp. 5401–5416, 2013.

[28] M. M. Naghsh and M. Modarres-Hashemi, "Exact theoretical performance analysis of optimum detector for statistical MIMO radars," *IET Journal on Radar, Sonar, and Navigation*, vol. 6, pp. 99–111, 2012.

[29] T. Kailath, "The divergence and Bhattacharyya distance measures in signal selection," *IEEE Trans. Commun.*, vol. 15, pp. 52–60, Feb. 1967.

[30] S. M. Kay, "Waveform design for multistatic radar detection," *IEEE Trans. Aerosp. Electron. Syst.*, vol. 45, pp. 1153–1165, Jul. 2009.

[31] A. Ben-Tal and A. Nemirovski, *Lectures on Modern Convex Optimization*. Philadelphia: SIAM, 2001.

[32] P. Stoica, J. Li, and X. Zhu, "Waveform synthesis for diversity-based transmit beampattern design," *IEEE Trans. Signal Process.*, vol. 56, no. 6, pp. 2593 –2598, Jun. 2008.

[33] P. Stoica and R. Moses, *Spectral Analysis of Signals*. New Jersey: Prentice Hall, 2005. [Online]. Available: http://user.it.uu.se/ ps/ref.html

[34] S. Boyd and L. Vanderberghe, *Convex Optimization*. Cambridge University Press, 2004.

[35] M. M. Naghsh, M. Soltanalian, P. Stoica, M. Modarres-Hashemi, A. De Maio, and A. Aubry, "A Doppler robust design of transmit sequence and receive filter in the presence of signal-dependent interference," *IEEE Trans. Signal Process.*, In Press, 2013.

[36] T. Roh and L. Vandenberghe, "Discrete transforms, semidefinite programming, and sum-of-squares representation of nonnegative polynomials," *SIAM Journal on Optimization*, vol. 16, no. 4, pp. 939–964, 2006.

[37] J. Benedetto, I. Konstantinidis, and M. Rangaswamy, "Phase-coded waveforms and their design," *IEEE Signal Process. Mag.*, vol. 26, no. 1, pp. 22 –31, Jan. 2009.

[38] M. Soltanalian and P. Stoica, "Designing unimodular codes via quadratic optimization," *IEEE Trans. Signal Process.*, Submitted, 2013.

[39] M. Soltanalian, B. Tang, J. Li, and P. Stoica, "Joint design of the receive filter and transmit sequence for active sensing," *IEEE Signal Process. Lett.*, vol. 20, no. 5, pp. 423–426, 2013.

[40] J. A. Tropp, I. S. Dhillon, R. W. Heath, and T. Strohmer, "Designing structured tight frames via an alternating projection method," *IEEE Trans. Inf. Theory*, vol. 51, no. 1, pp. 188–208, Jan. 2005.

[41] M. Skolnik, *Radar Handbook*, 3rd ed. New York: McGraw-Hill, 2008.

[42] M. Grant and S. Boyd. (2012, February) CVX package. [Online]. Available: http://www.cvxr.com/cvx

[43] M. Nayebi, M. Aref, and M. Bastani, "Detection of coherent radar signals with unknown doppler shift," *IEE Proceedings-Radar, Sonar and Navigation*, vol. 143, no. 2, pp. 79–86, 1996.

[44] J. Li, P. Stoica, and Z. Wang, "Doubly constrained robust Capon beamformer," *IEEE Trans. Signal Process.*, vol. 52, no. 9, pp. 2407 – 2423, Sep. 2004.
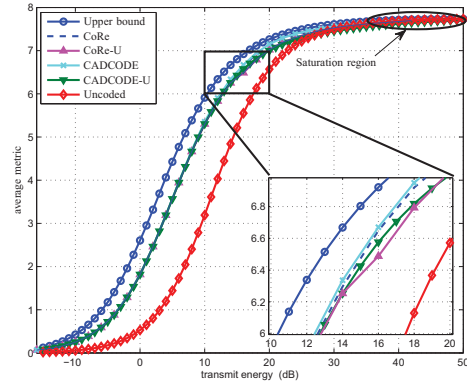
(a)
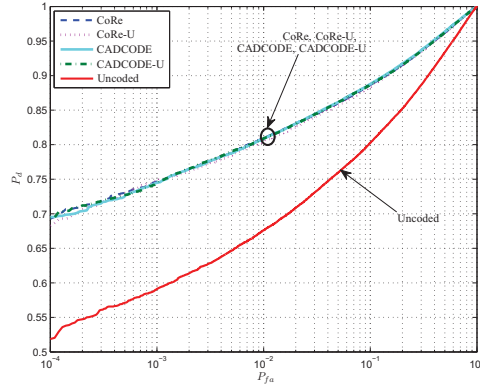
(b)
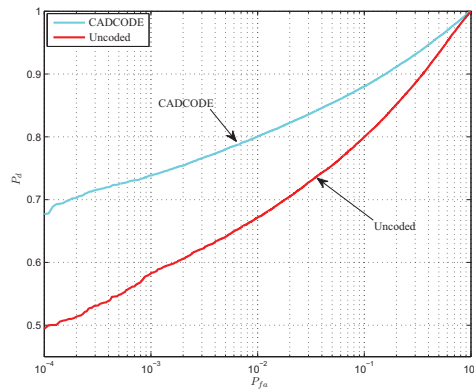
(c)

Fig. 1. The design of optimized codes of length $N = 16$ using the average metric. (a) depicts the average metric for different methods as well as the uncoded system vs. the transmit energy. (b) plots the ROC of the optimal detector associated with the same codes (as in sub-figure (a)) with $\sigma_T^2 = 10$ and $e = 10$. (c) depicts the ROC of the GLR detector (67) for the coded system (CADCODE) and uncoded one.
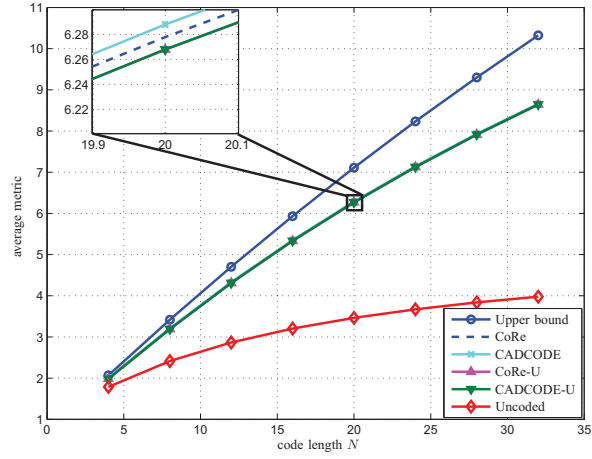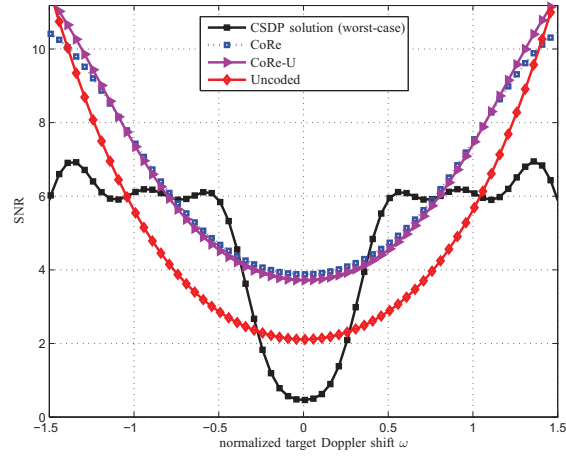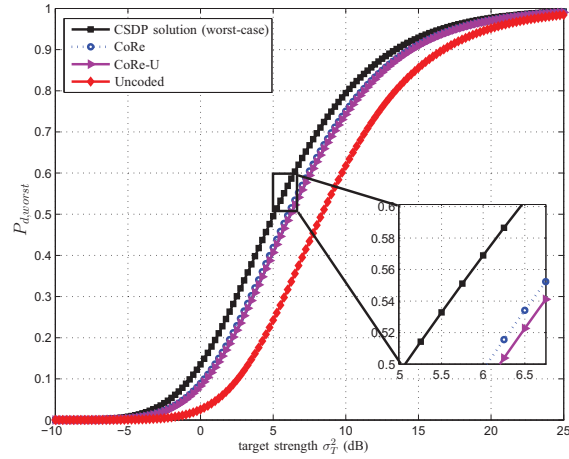
Fig. 2. The average metric associated with the upper bound (i.e. the CSDP solution in (25)), CoRe, CADCODE, CoRe-U, CADCODE-U, and the uncoded system vs. the code length N. A transmit energy of $e = 10$ was considered.

(a)

(b)

Fig. 3.   (a) The SNR for the CSDP solution, CoRe, CoRe-U, and the uncoded system vs. the normalized target Doppler shift for $N = 16$ and $e = 10$. (b) The worst-case detection probability of the CSDP solution, CoRe, CoRe-U, and the uncoded system vs. the target strength σ_T^2 for the same designs as in sub-figure (a).
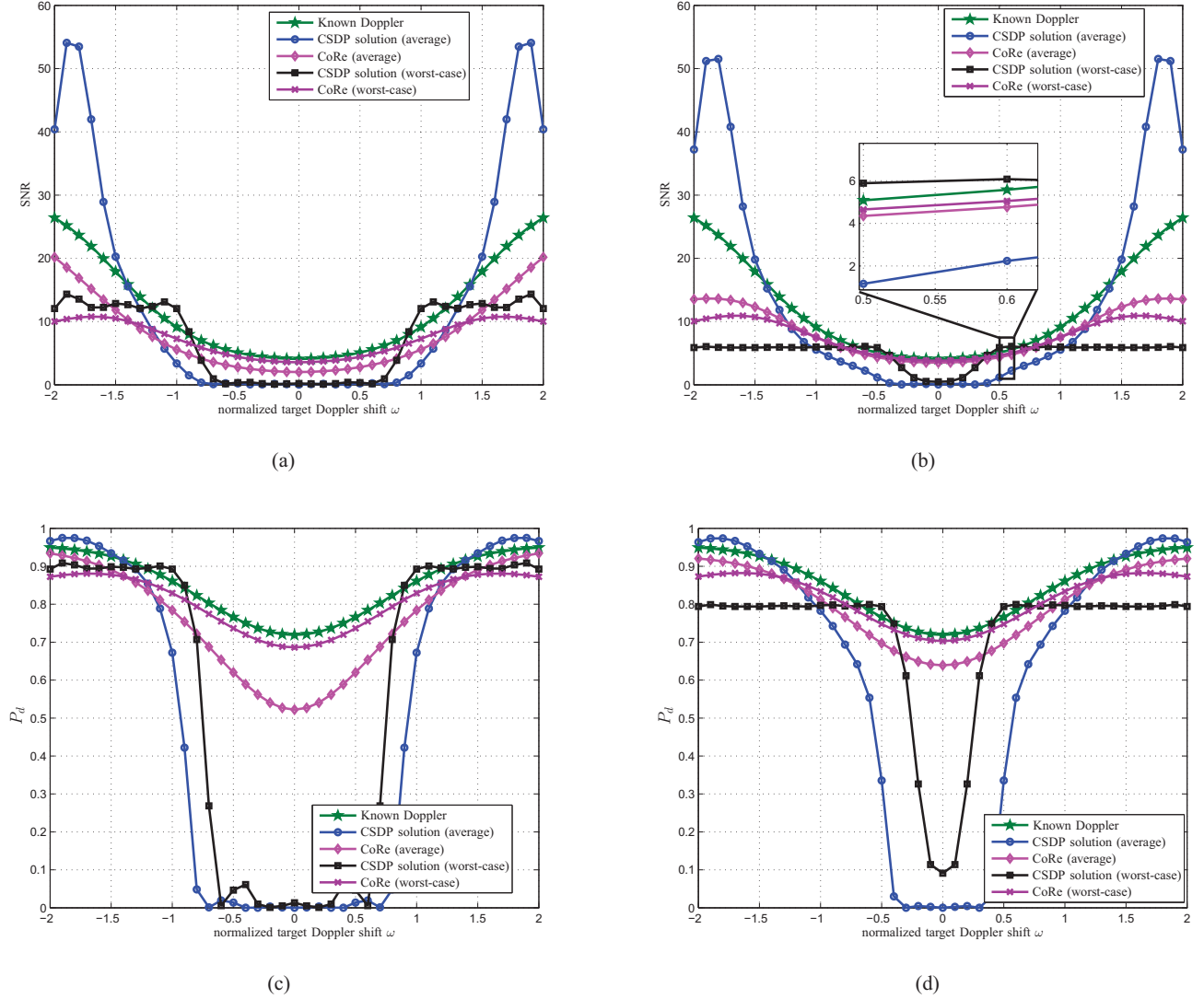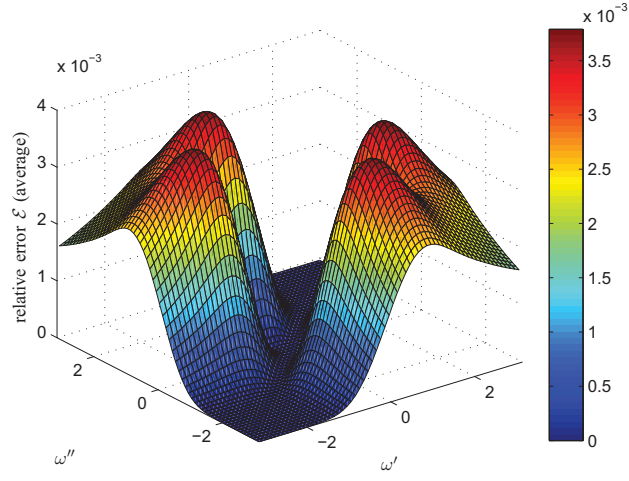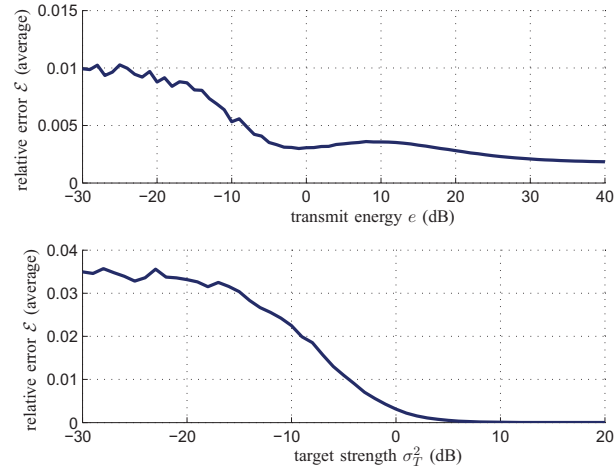
(a)

(b)

(c)

(d)

Fig. 4. Comparison of the average and worst-case code design approaches for $N = 16$, $e = 10$, and two different normalized target Doppler shift intervals Ω: (a) the SNR for $[-2, -1] \cup [1, 2]$ ($\sigma_T^2 = 1$), (b) the SNR for $[-2, -0.5] \cup [0.5, 2]$ ($\sigma_T^2 = 1$), (c) the detection probability for $[-2, -1] \cup [1, 2]$ ($\sigma_T^2 = 10$), and (d) the detection probability for $[-2, -0.5] \cup [0.5, 2]$ ($\sigma_T^2 = 10$).

(a)

(b)

Fig. 5.   A numerical analysis of the tightness of the lower bound $\mathcal{J}_{LB}$ on the J-divergence. (a) plots the average relative error $\mathcal{E}$ for various intervals of $\omega = [\min(\omega', \omega''), \max(\omega', \omega'')]$. (b) depicts the behavior of the average relative error $\mathcal{E}$ versus transmit energy e and target strength σ_T^2.